On the other hand, recent studies have shown the important role of $CD4^+$ helper T cells in optimal function and proliferation of $CD8^+$ T cells.[46] Therefore, the lack of $CD4^+$ helper T cells or anergic $CD4^+$ T cells may explain the limited TAA-specific $CD8^+$ T-cell responses in HCC. Further studies using $CD4^+$ T-cell-depleted PBMCs or $CD8^+$ T cells expanded with TAA-derived peptide may enable identification of more immunogenic HCC-specific TAAs and their epitopes.

In conclusion, the results of this study suggest that CypB, SART2, SART3, p53, MRP3, AFP, and hTERT are promising TAAs in HCC immunotherapy, that the administration of these TAAs or peptides containing their epitopes as vaccines after HCC treatment is likely to be effective, and that the concomitant use of anti-CTLA-4 antibodies may further increase antitumor immunity. We believe that the results of this study provide useful information for the development of immunotherapy for HCC.

Acknowledgment: The authors thank Kazumi Fushimi, Maki Kawamura, Masayo Baba and Nami Nishiyama for technical assistance.

References

1. Deuffic S, Poynard T, Buffat L, Valleron AJ. Trends in primary liver cancer. Lancet 1998;351:214-215.
2. Parkin DM, Bray F, Ferlay J, Pisani P. Estimating the world cancer burden: Globocan 2000. Int J Cancer 2001;94:153-156.
3. Lencioni R. Loco-regional treatment of hepatocellular carcinoma. HEPATOLOGY 2010;52:762-773.
4. Okuwaki Y, Nakazawa T, Shibuya A, Ono K, Hidaka H, Watanabe M, et al. Intrahepatic distant recurrence after radiofrequency ablation for a single small hepatocellular carcinoma: risk factors and patterns. J Gastroenterol 2008;43:71-78.
5. Nishizaka S, Gomi S, Harada K, Oizumi K, Itoh K, Shichijo S. A new tumor-rejection antigen recognized by cytotoxic T lymphocytes infiltrating into a lung adenocarcinoma. Cancer Res 2000;60:4830-4837.
6. Kawano K, Gomi S, Tanaka K, Tsuda N, Kamura T, Itoh K, et al. Identification of a new endoplasmic reticulum-resident protein recognized by HLA-A24-restricted tumor-infiltrating lymphocytes of lung cancer. Cancer Res 2000;60:3550-3558.
7. Gomi S, Nakao M, Niiya F, Imamura Y, Kawano K, Nishizaka S, et al. A cyclophilin B gene encodes antigenic epitopes recognized by HLA-A24-restricted and tumor-specific CTLs. J Immunol 1999;163:4994-5004.
8. Harashima N, Tanaka K, Sasatomi T, Shimizu K, Miyagi Y, Yamada A, et al. Recognition of the Lck tyrosine kinase as a tumor antigen by cytotoxic T lymphocytes of cancer patients with distant metastases. Eur J Immunol 2001;31:323-332.
9. Fujie T, Tahara K, Tanaka F, Mori M, Takesako K, Akiyoshi T. A MAGE-1-encoded HLA-A24-binding synthetic peptide induces specific anti-tumor cytotoxic T lymphocytes. Int J Cancer 1999;80:169-172.
10. Nishiyama T, Tachibana M, Horiguchi Y, Nakamura K, Ikeda Y, Takesako K, et al. Immunotherapy of bladder cancer using autologous dendritic cells pulsed with human lymphocyte antigen-A24-specific MAGE-3 peptide. Clin Cancer Res 2001;7:23-31.
11. Kikuchi M, Nakao M, Inoue Y, Matsunaga K, Shichijo S, Yamana H, et al. Identification of a SART-1-derived peptide capable of inducing HLA-A24-restricted and tumor-specific cytotoxic T lymphocytes. Int J Cancer 1999;81:459-466.
12. Nakao M, Shichijo S, Imaizumi T, Inoue Y, Matsunaga K, Yamada A, et al. Identification of a gene coding for a new squamous cell carcinoma antigen recognized by the CTL. J Immunol 2000;164:2565-2574.
13. Yang D, Nakao M, Shichijo S, Sasatomi T, Takasu H, Matsumoto H, et al. Identification of a gene coding for a protein possessing shared tumor epitopes capable of inducing HLA-A24-restricted cytotoxic T lymphocytes in cancer patients. Cancer Res 1999;59:4056-4063.
14. Tanaka H, Tsunoda T, Nukaya I, Sette A, Matsuda K, Umano Y, et al. Mapping the HLA-A24-restricted T-cell epitope peptide from a tumour-associated antigen HER2/neu: possible immunotherapy for colorectal carcinomas. Br J Cancer 2001;84:94-99.
15. Eura M, Chikamatsu K, Katsura F, Obata A, Sobao Y, Takiguchi M, et al. A wild-type sequence p53 peptide presented by HLA-A24 induces cytotoxic T lymphocytes that recognize squamous cell carcinomas of the head and neck. Clin Cancer Res 2000;6:979-986.
16. Umano Y, Tsunoda T, Tanaka H, Matsuda K, Yamaue H, Tanimura H. Generation of cytotoxic T-cell responses to an HLA-A24 restricted epitope peptide derived from wild-type p53. Br J Cancer 2001;84:1052-1057.
17. Ferries E, Connan F, Pages F, Gaston J, Hagnere AM, Vieillefond A, et al. Identification of p53 peptides recognized by CD8(+) T lymphocytes from patients with bladder cancer. Hum Immunol 2001;62:791-798.
18. Yamada A, Kawano K, Koga M, Matsumoto T, Itoh K. Multidrug resistance-associated protein 3 is a tumor rejection antigen recognized by HLA-A2402-restricted cytotoxic T lymphocytes. Cancer Res 2001;61:6459-6466.
19. Mizukoshi E, Nakamoto Y, Tsuji H, Yamashita T, Kaneko S. Identification of alpha-fetoprotein-derived peptides recognized by cytotoxic T lymphocytes in HLA-A24+ patients with hepatocellular carcinoma. Int J Cancer 2006;118:1194-1204.
20. Mizukoshi E, Nakamoto Y, Marukawa Y, Arai K, Yamashita T, Tsuji H, et al. Cytotoxic T-cell responses to human telomerase reverse transcriptase in patients with hepatocellular carcinoma. HEPATOLOGY 2006;43:1284-1294.
21. Ribas A, Butterfield LH, Glaspy JA, Economou JS. Current developments in cancer vaccines and cellular immunotherapy. J Clin Oncol 2003;21:2415-2432.
22. Rosenberg SA, Yang JC, Schwartzentruber DJ, Hwu P, Marincola FM, Topalian SL, et al. Immunologic and therapeutic evaluation of a synthetic peptide vaccine for the treatment of patients with metastatic melanoma. Nat Med 1998;4:321-327.
23. Itoh K, Yamada A. Personalized peptide vaccines: a new therapeutic modality for cancer. Cancer Sci 2006;97:970-976.
24. Butterfield LH, Ribas A, Meng WS, Dissette VB, Amarnani S, Vu HT, et al. T-cell responses to HLA-A*0201 immunodominant peptides derived from alpha-fetoprotein in patients with hepatocellular cancer. Clin Cancer Res 2003;9:5902-5908.
25. Butterfield LH, Ribas A, Dissette VB, Lee Y, Yang JQ, De la Rocha P, et al. A phase I/II trial testing immunization of hepatocellular carcinoma patients with dendritic cells pulsed with four alpha-fetoprotein peptides. Clin Cancer Res 2006;12:2817-2825.
26. Butterfield LH. Recent advances in immunotherapy for hepatocellular cancer. Swiss Med Wkly 2007;137:83-90.
27. Dougan M, Dranoff G. Immune therapy for cancer. Annu Rev Immunol 2009;27:83-117.
28. O'Day SJ, Maio M, Chiarion-Sileni V, Gajewski TF, Pehamberger H, Bondarenko IN, et al. Efficacy and safety of ipilimumab monotherapy in patients with pretreated advanced melanoma: a multicenter single-arm phase II study. Ann Oncol 2010;21:1712-1717.
29. Araki T, Itai Y, Furui S, Tasaka A. Dynamic CT densitometry of hepatic tumors. AJR Am J Roentgenol 1980;135:1037-1043.

30. Japan. LCSGo. Classification of primary liver cancer. English ed 2. Tokyo: Kanehara; 1997.
31. Desmet VJ, Gerber M, Hoofnagle JH, Manns M, Scheuer PJ. Classification of chronic hepatitis: diagnosis, grading and staging. HEPATOLOGY 1994;19:1513-1520.
32. Ikeda-Moore Y, Tomiyama H, Miwa K, Oka S, Iwamoto A, Kaneko Y, et al. Identification and characterization of multiple HLA-A24-restricted HIV-1 CTL epitopes: strong epitopes are derived from V regions of HIV-1. J Immunol 1997;159:6242-6252.
33. Kurokohchi K, Arima K, Nishioka M. A novel cytotoxic T-cell epitope presented by HLA-A24 molecule in hepatitis C virus infection. J Hepatol 2001;34:930-935.
34. Kuzushima K, Hayashi N, Kimura H, Tsurumi T. Efficient identification of HLA-A*2402-restricted cytomegalovirus-specific CD8(+) T-cell epitopes by a computer algorithm and an enzyme-linked immunospot assay. Blood 2001;98:1872-1881.
35. Oiso M, Eura M, Katsura F, Takiguchi M, Sobao Y, Masuyama K, et al. A newly identified MAGE-3-derived epitope recognized by HLA-A24-restricted cytotoxic T lymphocytes. Int J Cancer 1999;81:387-394.
36. Takahashi T, Tagami T, Yamazaki S, Uede T, Shimizu J, Sakaguchi N, et al. Immunologic self-tolerance maintained by CD25(+)CD4(+) regulatory T cells constitutively expressing cytotoxic T lymphocyte-associated antigen 4. J Exp Med 2000;192:303-310.
37. Zerbini A, Pilli M, Penna A, Pelosi G, Schianchi C, Molinari A, et al. Radiofrequency thermal ablation of hepatocellular carcinoma liver nodules can activate and enhance tumor-specific T-cell responses. Cancer Res 2006;66:1139-1146.
38. Ayaru L, Pereira SP, Alisa A, Pathan AA, Williams R, Davidson B, et al. Unmasking of alpha-fetoprotein-specific CD4(+) T-cell responses in hepatocellular carcinoma patients undergoing embolization. J Immunol 2007;178:1914-1922.
39. Sallusto F, Lenig D, Forster R, Lipp M, Lanzavecchia A. Two subsets of memory T lymphocytes with distinct homing potentials and effector functions. Nature 1999;401:708-712.
40. Peggs KS, Quezada SA, Chambers CA, Korman AJ, Allison JP. Blockade of CTLA-4 on both effector and regulatory T cell compartments contributes to the antitumor activity of anti-CTLA-4 antibodies. J Exp Med 2009;206:1717-1725.
41. Zerbini A, Pilli M, Soliani P, Ziegler S, Pelosi G, Orlandini A, et al. Ex vivo characterization of tumor-derived melanoma antigen encoding gene-specific CD8+cells in patients with hepatocellular carcinoma. J Hepatol 2004;40:102-109.
42. Gehring AJ, Ho ZZ, Tan AT, Aung MO, Lee KH, Tan KC, et al. Profile of tumor antigen-specific CD8 T cells in patients with hepatitis B virus-related hepatocellular carcinoma. Gastroenterology 2009;137:682-690.
43. Fujioka M, Nakashima Y, Nakashima O, Kojiro M. Immunohistologic study on the expressions of alpha-fetoprotein and protein induced by vitamin K absence or antagonist II in surgically resected small hepatocellular carcinoma. HEPATOLOGY 2001;34:1128-1134.
44. Hussain SP, Schwank J, Staib F, Wang XW, Harris CC. TP53 mutations and hepatocellular carcinoma: insights into the etiology and pathogenesis of liver cancer. Oncogene 2007;26:2166-2176.
45. Fu J, Xu D, Liu Z, Shi M, Zhao P, Fu B, et al. Increased regulatory T cells correlate with CD8 T-cell impairment and poor survival in hepatocellular carcinoma patients. Gastroenterology 2007;132:2328-2339.
46. Kennedy R, Celis E. Multiple roles for CD4+ T cells in anti-tumor immune responses. Immunol Rev 2008;222:129-144.

ARTICLE

BIOTECHNOLOGY AND BIOENGINEERING

Saturation of Transgene Protein Synthesis From mRNA in Cells Producing a Large Number of Transgene mRNA

Yuki Takahashi, Makiya Nishikawa, Naomi Takiguchi, Tetsuya Suehara, Yoshinobu Takakura

Department of Biopharmaceutics and Drug Metabolism, Graduate School of Pharmaceutical Sciences, Kyoto University, Kyoto 606-8501, Japan; telephone: +81-75-753-4580; fax: +81-75-753-4614; e-mail: makiya@pharm.kyoto-u.ac.jp

Received 21 December 2010; revision received 4 March 2011; accepted 11 April 2011

Published online 21 April 2011 in Wiley Online Library (wileyonlinelibrary.com). DOI 10.1002/bit.23179

ABSTRACT: Experimental results have suggested that transgene expression can be saturated when large amounts of plasmid vectors are delivered into cells. To investigate this saturation kinetic behavior, cells were transfected with monitoring and competing plasmids using cationic liposomes. Even although an identical amount of a monitoring plasmid expressing firefly luciferase (FL) was used for transfection, transgene expression from the plasmid was greatly affected by the level of transgene expression from competing plasmids expressing renilla luciferase (RL). Similar results were obtained by exchanging the monitoring and competing plasmids. The competing plasmid-dependent reduction in transgene expression from the monitoring plasmid was also observed in mouse liver after hydrodynamic injection of plasmids. On the other hand, the mRNA and protein expression level of glyceraldehyde-3-phosphate dehydrogenase (GAPDH), an endogenous gene, in the liver hardly changed even when transgene expression process is saturated. The expression of FL from a monitoring plasmid was significantly restored by siRNA-mediated degradation of RL mRNA that was expressed from a competing plasmid. These results suggest that the efficiency of protein synthesis from plasmid vectors is reduced when a large amount of mRNA is transcribed with no significant changes in endogenous gene expression.

Biotechnol. Bioeng. 2011;108: 2380–2389.

KEYWORDS: saturation; transgene expression; plasmid vector; mRNA expression; RNA interference

Correspondence to: M. Nishikawa

Contract grant sponsor: Ministry of Education, Science, Sports, and Culture of Japan
Contract grant sponsor: Ministry of Health, Labour, and Welfare of Japan
Contract grant sponsor: Program for Promotion of Fundamental Studies in Health Sciences of the National Institute of Biomedical Innovation (NIBIO)

Introduction

Development of efficient gene delivery methods is needed not only for gene therapy but also for the functional studies of genes. Of the various vectors and gene delivery/transfer methods developed thus far, rapid injection of naked plasmid DNA in a large volume of isotonic solution, the so-called the hydrodynamic injection method, is one of the most effective and promising gene delivery methods because of its simplicity, reproducibility, and high efficiency (Herweijer and Wolff, 2007; Kobayashi et al., 2005; Lewis and Wolff, 2007; Liu et al., 1999). Therefore, this gene delivery technique has frequently been used as an experimental tool to investigate the gene of interest in mouse liver, the organ that most efficiently expresses the gene products after hydrodynamic delivery of naked plasmid DNA.

In a previous study, we found, using a firefly luciferase (FL)-expressing plasmid DNA, that the level of luciferase activity in mouse liver increased in parallel with the increasing dose of the plasmid up to about 1 μg DNA/mouse (Kobayashi et al., 2004). However, we also noticed that the luciferase activity reached a plateau at doses around 10 μg DNA/mouse, suggesting that the transgene expression from plasmid DNA is saturated at such high doses. These experimental results could be explained by assuming the presence of one or more saturable processes in the transgene expression after hydrodynamic delivery of plasmid DNA to mouse liver. One obvious possibility is that the amount of plasmid DNA delivered to the nucleus of transfected cells is not proportional to the increasing dose of the DNA. However, this can be rejected by the previous finding that 20 μg empty plasmid co-administered had no significant effect on the level of transgene expression from 0.2 μg luciferase-expressing plasmid (Kobayashi et al., 2004). The empty plasmid used contained the same promoter/enhancer and other components as those in the luciferase-expressing plasmid except for the cDNA region. Therefore, these results

strongly support the hypothesis that the efficiency of the cellular uptake and intracellular trafficking of plasmid DNA, including the nuclear entry, is not a function of the amount or concentration of the DNA, even although several reports have indicated that transcription factors and other proteins were involved in the nuclear entry of plasmid DNA microinjected into the cytosol (Dean, 1997; Dean et al., 1999; Miller and Dean, 2008).

There are several steps in the process of transgene expression, including RNA synthesis (transcription), RNA modification (splicing), export of mRNA from the nucleus into the cytosol, protein synthesis (translation), post-translational modification of protein, and transport/trafficking of protein. Considering the fact that all these steps in the gene expression are capacity-limited, it is reasonable that transgene expression becomes saturated when a large amount of DNA is introduced into cells. In good agreement with this hypothesis, saturation in transgene expression has been discussed in several studies involving transgene expression in cultured cells. Tachibana et al. (2002) investigated the relationship between the dose of plasmid DNA added to cells and the amount of transgene product. They showed that the copy number of plasmid DNA in the nucleus correlated with its dose. Furthermore, they demonstrated that the copy number in the nucleus did not correlate with the amount of transgene product, especially when the copy number was high. A recent study by Cohen et al. (2009) also showed that nuclear uptake of plasmid DNA was linearly related to its dose whereas the level of transgene expression was not. Carpentier et al. (2007) investigated the limiting factors involved in the process of transgene expression. They found that both transcriptional and translational processes were saturated under optimal transfection conditions in which quite a high level of gene expression was obtained. These previous studies strongly suggest that transgene expression can be saturated under certain conditions.

Detailed understanding of this saturable mechanism of transgene expression from plasmid vectors will provide new insights into how gene expression is regulated in cells. The understanding could also lead to the development of methods to achieve high level of transgene expression without saturation. In addition, from the viewpoint of safety, it is important to investigate whether endogenous gene expression is affected when transgene expression process is saturated, because it may cause unexpected side effects, such as cell death. For example, Lin et al. (2007) reported that adenoviral vector-mediated high transgene expression of serum response factor resulted in nonspecific reduction of transcription of endogenous genes and caused cell death. Therefore, in the present study, we examined whether the synthesis of transgene products is actually saturated when a large amount of plasmid DNA is delivered to cells. To this end, cultured cells were transfected with two types of plasmid vectors, each of which encodes a reporter protein, and transgene expression from the vectors was used to investigate whether the expression from one plasmid (monitoring plasmid) is affected by that from the other plasmid (competing plasmid). Then, similar experiments were carried out using mice that received a hydrodynamic injection of the two plasmid vectors. In addition, the mRNA and protein levels of glyceraldehyde-3-phosphate dehydrogenase (GAPDH) in mouse liver were evaluated as a model endogenous gene to evaluate the effect of transgene expression on endogenous gene expression. Small interfering RNA (siRNA) was used to reduce the amount of mRNA without altering the amount of plasmids for transfection.

Materials and Methods

Plasmid DNA and siRNA

Salmon testes DNA (stDNA) was purchased from Sigma (St Louis, MO). Plasmid DNA encoding FL under the control of CMV promoter (pFL-CMV) was constructed as described previously (Nomura et al., 1999). The following plasmids were purchased from the sources in brackets: pGL3-control vector (Promega, Madison, WI), pLuc-mcs (Stratagene, La Jolla, CA), pRL-CMV (Promega) encoding renilla luciferase (RL) under the control of CMV promoter, pRL-SV40 (Promega), pRL-TK (Promega), pEGFP-F (BD Biosciences Clontech, Palo Alto, CA) encoding farnesylated enhanced green fluorescent protein (GFP) under the control of CMV promoter. These plasmids were renamed according to the cDNA and promoter of each plasmid as follows: pFL-SV40, pFL-TATA, pRL-CMV, pRL-SV40, pRL-TK, and pGFP-CMV. siRNA targeting RL mRNA (siRL) or GFP mRNA (siGFP) was purchased from Takara Bio (Otsu, Japan). Target sites in the RL and GFP mRNA are as follows: RL, 5′-GUAGCGCGGUGUAUUAUAC-3′; GFP, 5′-GGCUAC-GUCCAGGAGCGCA-3′.

Cell Culture

A murine melanoma cell line, B16-BL6, was obtained from the Cancer Chemotherapy Center of the Japanese Foundation for Cancer Research (Poste et al., 1980). B16-BL6 cells were cultured in Dulbecco's modified Eagle's minimum essential medium (Nissui Pharmaceutical, Tokyo, Japan) supplemented with 10% fetal bovine serum and penicillin (100 U/mL)/streptomycin (100 μg/mL)/L-glutamine (2 mM) at 37°C and 5% CO_2.

In vitro Transfection

B16-BL6 cells were plated on 24-well culture plates at the density of 2×10^4 cells/well. After an overnight incubation, transfection of plasmid DNA was carried out using Lipofectamine 2000 (Invitrogen, Carlsbad, CA) according to the manufacturer's instructions. In brief, 1 μg of nucleic acids (plasmids with or without siRNA), was mixed with 3 μg Lipofectamine 2000 in Opti-MEM I (Invitrogen) at a

final concentration of 6 μg Lipofectamine 2000 mL^{-1}. The resulting complex was added to cells and the cells were incubated with the complex for 4 h. Then, cells were washed with PBS and further incubated with the culture medium.

Luciferase Assay in B16-BL6 Cells

B16-BL6 cells were lysed using the cell lysis buffer of an assay kit (PiccageneDual, Toyo Ink, Tokyo, Japan). Then, samples were mixed with the kit luciferase assay buffer, and the chemiluminescence produced was measured in a luminometer (Lumat LB9507, EG and G Berthold, Bad Wildbad, Germany). The luciferase activities were converted to the amount of firefly and RL using recombinant proteins as the standard.

Flow Cytometric Analysis of GFP Expression in B16-BL6 Cells

B16-BL6 cells were transfected with pGFP-CMV as described above. One day after transfection, adherent cells were detached by trypsinization and resuspended in PBS. Resuspended cells were analyzed on a flow cytometer (FACSCan, BD, Franklin Lakes, NJ). The threshold on FSC was set to exclude cell debris without excluding any populations of interest.

mRNA Quantification in B16-BL6 Cells

One day after transfection, total RNA was extracted from cells using Sepasol RNA I super (Nacalai Tesque, Kyoto, Japan). Following RNase-free DNase I treatment (Takara Bio), reverse transcription was performed using a SuperScript II (Invitrogen) and dT-primer according to the manufacturer's protocol. For a quantitative analysis of mRNA expression, real-time PCR was carried out with total cDNA using a Light-Cycler instrument (Roche Diagnostics, Basle, Switzerland) as reported previously (Takahashi et al., 2005). The mRNA expression of target genes was normalized using the mRNA level of GAPDH.

Animal Experiments

Four-week-old male ICR mice (approximately 20 g body weight), purchased from Japan SLC, Inc. (Shizuoka, Japan) were used for all experiments. The protocols for animal experiments were approved by the Animal Experimentation Committee of the Graduate School of Pharmaceutical Sciences of Kyoto University. Mice received an intravenous injection of plasmid DNA by the hydrodynamic injection method as described previously (Liu et al., 1999). At 6 h after gene transfer, the peak time of the expression of firefly and RLs from the plasmid vectors used, the mice were killed by cervical dislocation and the amount of luciferase mRNA and protein in the liver was determined as described below.

Quantification of the Amounts of Luciferase and GAPDH in Mouse Liver

The liver was excised and homogenized in a lysis buffer (0.1 M Tris (pH 7.8), 0.05% Triton X-100, 2 mM EDTA, 0.1% protease inhibitor cocktail (Sigma)), and centrifuged at 13,000*g* for 20 min at 4°C. The amount of luciferase in the supernatant was determined by the method described in the above section. The amount of GAPDH protein in the lysate was measured by ELISA by using a commercial kit (GAPDH Whole-cell Normalization kit, Active Motif, Carlsbad, CA).

mRNA Quantification in Mouse Liver

Total RNA was extracted from approximately 50 mg liver samples using Sepasol RNA I Super. After purification of the extracted RNA sample using an RNeasy mini kit (Qiagen, Hilden, Germany), reverse transcription and real-time PCR analysis were performed as described in the above section.

Statistical Analysis

The normality of the data was evaluated by using Shapiro–Wilk test. Data of normal distribution were analyzed by Student's *t*-test for two independent samples or one-way analysis of variance (ANOVA) followed by the Tukey's test for multiple comparisons. Data without normal distribution were analyzed using Mann–Whitney rank sum test for two independent samples or Kruskal–Wallis one-way ANOVA on ranks followed by the Tukey's test for multiple comparisons. A *P*-value of less than 0.05 was considered to be statistically significant.

Results

Time-Course and Dose-Dependent Luciferase Expression in B16-BL6 Cells

Figure 1A shows the time-courses of the amounts of firefly and RLs in cells after cotransfection with pFL-CMV and pRL-CMV. The expression of both luciferases was detectable as early as 6 h after transfection, reached maximum values at 24 h and then eventually decreased with time. As the highest luciferase expression was detected at 24 h after transfection under the conditions used, this time point was selected and used in the following experiments to examine transgene expression in B16-BL6 cells.

Figure 1B shows the amount of FL in cells transfected with different amounts of pFL-TATA, pFL-SV40, or pFL-CMV. pFL-CMV showed the highest FL, followed by pFL-SV40, then pFL-TATA, reflecting the strength of these promoters used. When cells were transfected with one of the RL-expressing plasmid DNA, pRL-CMV showed the highest RL activity, followed by pRL-SV40 and pRL-TK (data not shown).

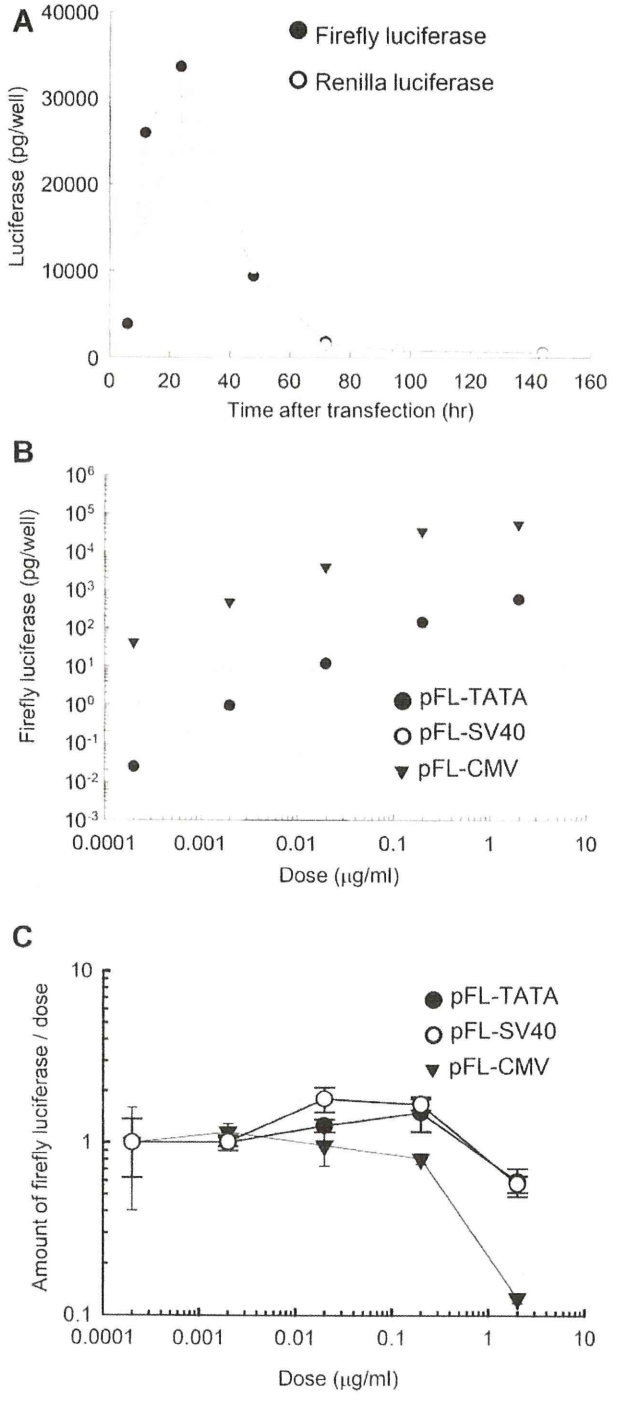

Figure 1. Time- and dose-dependent luciferase expression in B16-BL6 cells after transfection of luciferase-expressing plasmid DNA. **A**: The firefly (closed symbols) and renilla (open symbols) luciferase activities were measured at indicated times after transfection of B16-BL6 cells with 1 μg/mL pFL-CMV and 1 μg/mL pRL-CMV. The results are expressed as the mean ± SD ($n = 4$). **B**: The luciferase activity was measured at 1 day after transfection of B16-BL6 cells with the indicated dose of pFL-CMV (open triangle), pFL-SV40 (open circle), or pFL-TATA (closed circle). The results are expressed as the mean ± SD ($n = 3$). **C**: The amount of firefly luciferase protein in (B) was divided by the dose of plasmid DNA. The results are expressed as the mean ± SD of the relative value to that of 0.0002 μg/mL (pFL-CMV and pFL-SV40) or to that of 0.002 μg/mL (pFL-TATA) ($n = 3$).

To statistically evaluate whether the expression is saturated with an increasing amount of plasmid DNA, the expression efficiency was estimated by dividing the luciferase activity by the dose (Fig. 1C). The value was about 40,000 pg/well/μg plasmid DNA at the lowest dose of 0.0002 μg/mL pFL-CMV. Increasing the dose to 2 μg/mL significantly reduced the value to 5,000 pg/well/μg plasmid DNA.

Luciferase Expression in B16-BL6 Cells Transfected With Two Different Plasmids

Figure 2 shows the amounts of firefly (Fig. 2A) and RL (Fig. 2B) in cells 24 h after cotransfection with 1.8 μg/mL pFL-TATA, pFL-SV40, or pFL-CMV and 0.2 μg/mL pRL-TK, pRL-SV40, or pRL-CMV. The amount of FL was the highest in cells transfected with pFL-CMV, which was about 4- and 20-fold higher than that in cells transfected with pFL-SV40 or pFL-TATA, respectively. In all cases examined, the amount of FL was hardly affected by the cotransfection with renilla-expressing plasmid DNA (Fig. 2A). This was probably because the dose of the RL-expressing plasmid DNA was only a tenth of the total amount of plasmids used for transfection. In marked contrast, the RL activity in B16-BL6 cells was affected not only by the type of RL-expressing plasmid DNA, but also by the type of competing, FL expressing plasmid DNA (Fig. 2B). RL activity in cells transfected with pRL-CMV and pFL-CMV (pRL-CMV/pFL-CMV) or pRL-SV40/pFL-CMV was significantly lower than that in cells transfected with pRL-CMV/pFL-TATA or pRL-SV40/pFL-TATA, respectively. The amount of RL in B16-BL6 cells transfected with pRL-TK was quite low compared with cells transfected with pRL-CMV or pRL-SV40.

Similar experiments were performed using 0.2 μg/mL FL-expressing plasmid DNA and 1.8 μg/mL RL-expressing plasmid DNA (Fig. 2C and D). The amount of FL in cells cotransfected with pFL-CMV/pRL-CMV was significantly lower than that in cells cotransfected with pFL-CMV/pRL-TK (Fig. 2C). Again, the amount of RL was hardly affected by the type of FL expressing plasmid vectors cotransfected (Fig. 2D).

Fluorescent Histogram of GFP in B16-BL6 Cells Transfected With pGFP-CMV and Renilla Luciferase-Expressing Plasmid

Figure 2E shows typical histograms of the fluorescence intensity of B16-BL6 cells transfected with pGFP-CMV and one of the following plasmids: pRL-CMV, pRL-SV40, or pRL-TK. In all cases examined, there was a large variation in the level of fluorescence intensity of B16-Bl6 cells transfected with pGFP-CMV. There were no obvious differences in the histograms of cells transfected with pGFP-CMV/pRL-TK or pGFP-CMV/pRL-SV40. On the other hand, the histogram of cells transfected with pGFP-CMV/pRL-CMV was different from the others; the percentage of cells with a

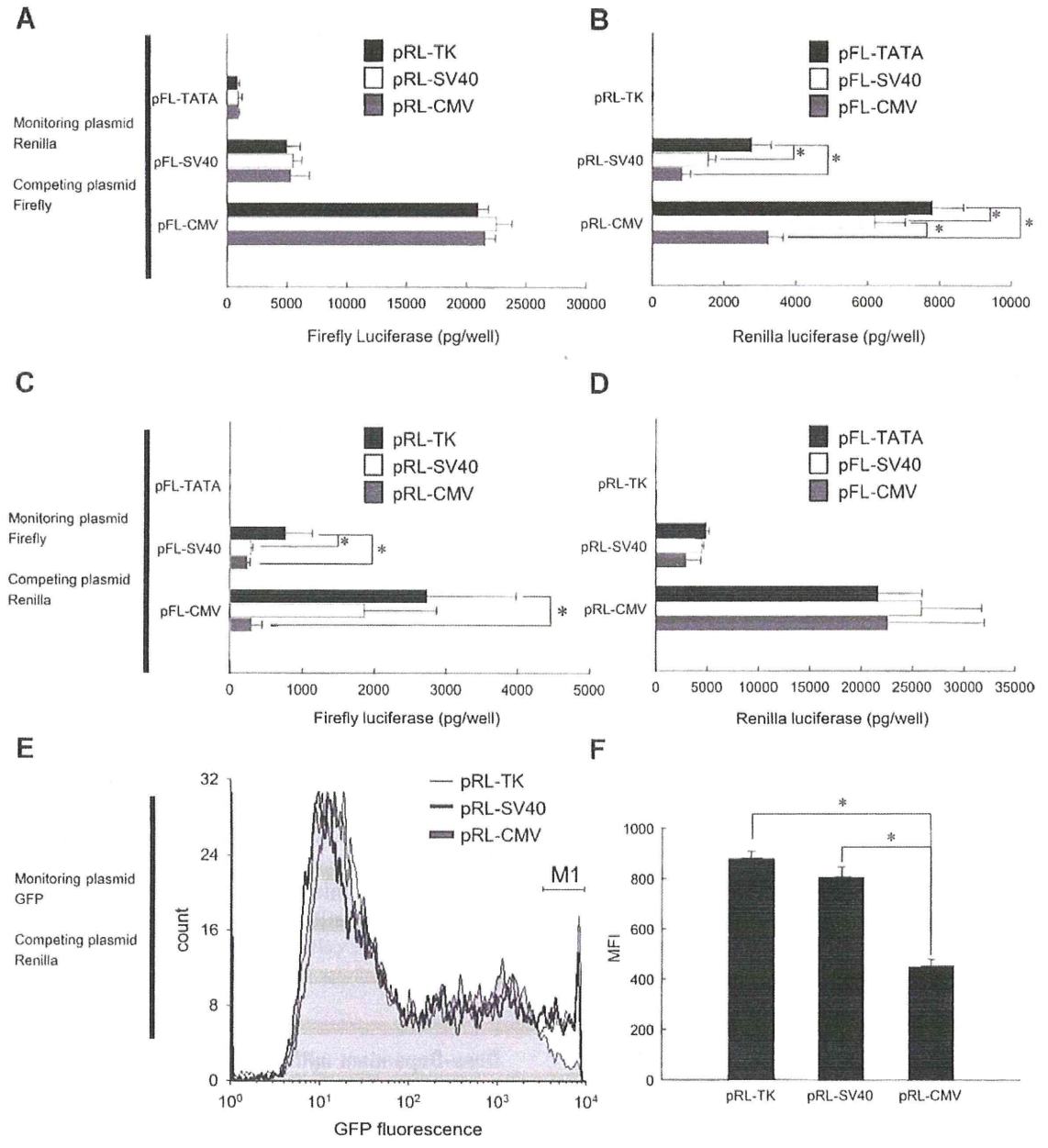

Figure 2. Effect of the level of transgene expression from competing plasmid DNA on transgene expression from monitoring plasmid DNA. **A and B**: B16-BL6 cells were cotransfected with 1.8 μg/mL pFL-TATA (closed bar), pFL-SV40 (open bar), or pFL-CMV (gray bar) and 0.2 μg/mL pRL-TK (closed bar), pRL-SV40 (open bar), or pRL-CMV (gray bar). One day after transfection, firefly (A) and renilla (B) luciferase activities were simultaneously measured. The results are expressed as the mean ± SD ($n = 4$). $^*P < 0.05$, compared with the pFL-TATA-transfected group. **C and D**: B16-BL6 cells were cotransfected with 1.8 μg/mL pRL-TK (closed bar), pRL-SV40 (open bar), or pRL-CMV (gray bar) and 0.2 μg/mL pFL-TATA (closed bar), pFL-SV40 (open bar), or pFL-CMV (gray bar). One day after transfection, firefly (C) and renilla (D) luciferase activities were simultaneously measured. The results are expressed as the mean ± SD ($n = 4$). $^*P < 0.05$ (vs. pRL-TK transfected group). **E and F**: B16-BL6 cells were cotransfected with 1.8 μg/mL pRL-CMV (line with shade), pRL-SV40 (bold line), or pRL-TK (solid line) and 0.2 μg/mL pGFP-CMV. One day after transfection, the fluorescence intensity histogram (E) and mean fluorescence intensity (F) of cells were analyzed by flow cytometry. The results are expressed as the mean ± SD ($n = 4$). $^*P < 0.05$.

high fluorescence intensity (the M1 region in the histogram) was 3%, and this value was smaller than the 8% and 9% for the pGFP-CMV/pRL-SV40- and pGFP/pRL-TK-treated cells, respectively. These findings indicate that cotransfection of cells with pRL-CMV, the plasmid with the strongest promoter among those used, markedly reduced the expression of GFP from pGFP-CMV only in cells that received efficient delivery of these two plasmids. In accordance with these histograms, the mean fluorescence intensity of cells transfected with pGFP-CMV/pRL-CMV

was significantly lower than that of cells transfected with pGFP-CMV/pRL-TK or pGFP-CMV/pRL-SV40 (Fig. 2F).

mRNA and Protein Expression Level of Luciferases in B16-BL6 Cells Transfected With Two Different Plasmids

The mRNA level was measured in B16-BL6 cells transfected with two types of plasmids, each of which expressed firefly or RL. Again, cells were transfected with 0.2 μg/mL pFL-CMV and 1.8 μg/mL RL-expressing plasmid, and the mRNA and luciferase activity were simultaneously measured at 24 h after transfection (Fig. 3). The amount of RL protein was dependent on the type of plasmids used as described above, but it was almost proportional to its mRNA level in all cases (Fig. 3A). The amount of FL protein was highly dependent on the type of RL-expressing plasmid cotransfected (Fig. 3B), as shown in Figure 2B. Moreover, the mRNA level of FL was also affected by other plasmids in a manner dependent on the promoter strength (Fig. 3B), suggesting that some processes leading to mRNA expression are saturated in cells that produce a large amount of mRNA. In addition, the degree of reduction in FL mRNA by cotransfection with pFL-CMV/pRL-CMV (about 20% of pFL-CMV/pRL-TK) was less than that of FL protein (about 8%), which implies that the amount of FL protein was disproportionate to its mRNA level.

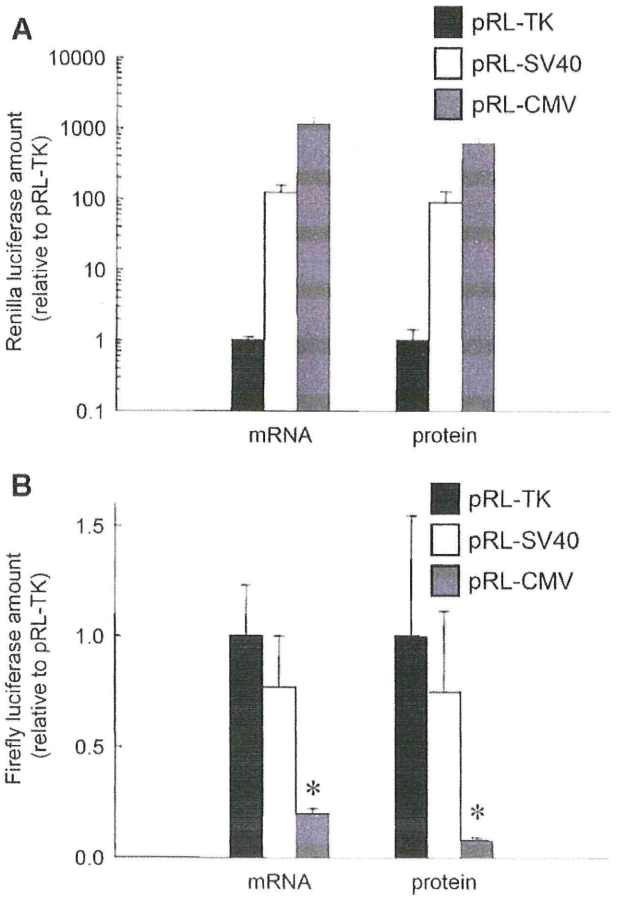

Figure 3. Effect of cotransfection on the levels of mRNA and protein in B16-BL6 cells. **A and B**: B16-BL6 cells were cotransfected with 1.8 μg/mL pRL-TK (closed bar), pRL-SV40 (open bar), or pRL-CMV (gray bar) and 0.2 μg/mL pFL-CMV. One day after transfection, mRNA and protein expression levels of renilla (A) and firefly (B) luciferase were simultaneously measured. The results are expressed as the mean ± SD ($n = 4$). $^*P < 0.05$.

Luciferase Expression in B16-BL6 Cells Transfected With siRNA and Plasmids

The results obtained thus far are consistent with the hypothesis that the synthesis of protein from mRNA is saturated when a large amount of mRNA is transcribed, and this leads to disproportionate protein synthesis to the mRNA level. To confirm this hypothesis, we degraded the mRNA of RL using siRL, an siRNA targeting RL, and measured the amount of luciferase proteins. For this purpose, B16-BL6 cells were cotransfected with 1 μg/mL siRL or siGFP, a control siRNA, in addition to 0.9 μg/mL pRL-CMV, pRL-SV40, or pRL-TK and 0.1 μg/mL pFL-CMV. As expected, the amount of RL was markedly suppressed in cells transfected with siRL compared with siGFP (Fig. 4A), which suggests that siRL successfully degraded the target mRNA under these experimental conditions. Cotransfection of siRL significantly increased the amount of FL in B16-BL6 cells transfected with pRL-CMV/pFL-CMV (Fig. 4B). These results suggest that siRNA-mediated degradation of mRNA from competing plasmids is effective in restoring transgene expression from the monitoring plasmid. However, the FL expression in the cells transfected with siRL, pFL-CMV, and pRL-CMV was lower than that of the cells transfected with siRL, pFL-CMV, and pRL-TK.

Dose-Dependent mRNA and Protein Expression of Luciferase in Mice After Hydrodynamics-Based Administration and its Effect on GAPDH Expression

Figure 5A shows the amounts of mRNA and protein of FL in mouse liver 6 h after hydrodynamic injection of pFL-CMV at different doses. Results were normalized to those of mice that received 1 μg/mouse pFL-CMV administration. A linear correlation was observed between the FL mRNA and the plasmid dose over the dose range investigated, that is, from 1–300 μg/mouse. At the dose of 10 μg/mouse, the relative amount of luciferase protein was comparable with that of mRNA expression, indicating that the efficiency of protein synthesis from mRNA was similar at doses of 1 and 10 μg/mouse. However, at a dose of 30 μg/mouse or higher, the ratio of FL protein to its mRNA was smaller than at the low doses. Thus, these results indicate that the amount of luciferase protein becomes disproportionate to the amount of its mRNA in mouse liver, when the mRNA level is

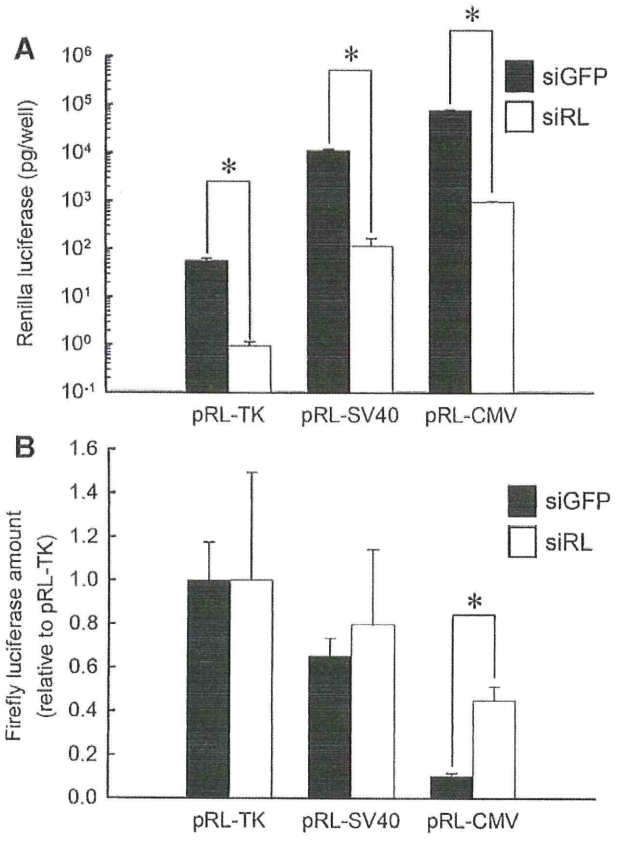

Figure 4. Effect of siRNA-mediated degradation of mRNA expressed from the competing plasmid on the expression from the monitoring plasmid. **A and B:** B16-BL6 cells were cotransfected with siGFP (closed bar) or siRL (open bar) (1 μg/mL), 0.9 μg/mL pRL-CMV, pRL-SV40, or pRL-TK and 0.1 μg/mL pFL-CMV. One day after transfection, renilla (A) and firefly (B) luciferase activities were simultaneously measured. The results are expressed as the mean ± SD ($n = 4$). $^*P < 0.05$.

increased. Then, the mRNA and protein amounts of FL were divided by the dose, and the values obtained were used to evaluate the efficiency or saturation of the expression. The efficiency of mRNA expression was not significantly affected by the dose, whereas that of protein expression significantly decreased with an increase in the dose of plasmid DNA.

To evaluate whether endogenous gene expression process is affected by large amount of mRNA expressed from plasmid vectors, the mRNA and protein expression of FL and GAPDH in mouse liver were simultaneously measured 6 h after hydrodynamic administration of 0, 1, or 100 μg pFL-CMV (Fig. 5B). As is the case of the experiment above, the difference in mRNA amount of FL between 1 and 100 μg was bigger than that in protein amount, which suggests the existence of saturation of protein synthesis process of transgene. No significant changes in GAPDH mRNA and protein expression were observed among all treatment group despite the fact that transgene expression process was saturated.

mRNA and Protein Expression of Luciferases in Mouse Liver After Hydrodynamic Injection of Naked Plamid Vectors

Finally, mice received a hydrodynamic injection of 1 μg pRL-CMV and 10 μg pFL-CMV, pFL-SV40, or pFL-TATA, and the levels of mRNA and protein were simultaneously measured (Fig. 5C and D). The amount of FL was dependent on the strength of promoter and proportional to its mRNA level (Fig. 5C). The mRNA level of RL was almost the same in all cases (Fig. 5D), reflecting the fact that the same amount of pRL-CMV was used for hydrodynamic injection. In contrast, the amount of RL protein in the liver of mice receiving pRL-CMV/pFL-CMV was significantly lower than that of mice receiving pRL-CMV/pFL-TATA (Fig. 5C).

Discussion

Transgene expression from monitoring plasmid was reduced by cotransfection with competing plasmid driven by a strong promoter and this phenomenon was independent of the type of cDNA encoded in the monitoring and competing plasmids (Fig. 2). These results suggest that saturation of transgene expression is not dependent on the type of transgene product. In the experiment using pGFP-CMV, cells with a very high fluorescence intensity, which was found after cotransfection of cells with pRL-SV40 or pRL-TK, were not detected when cells were cotransfected with pRL-CMV. The cells with high fluorescence intensity should have been delivered with a large amount of pGFP-CMV and, therefore, they could have also efficiently taken up coexisting plasmids. Therefore, it is reasonable to suggest that transgene expression is saturated especially in cells that encounter a large amount of plasmid DNA. Although the both experiments exhibited a similar trend, the degree of the reduction by co-transfection with pRL-CMV was much less in the GFP experiment than that in the luciferase experiment. The discrepancy may be explained by the difference in the detection sensitivity of GFP and luciferase expression.

Transgene expression from plasmid DNA requires a number of processes, such as delivery of plasmid DNA to the nucleus, mRNA transcription from the DNA, export of mRNA from the nucleus, processing of mRNA, translation, and post-translational modification of protein. In the present study, we found that the level of mRNA and protein expression from monitoring plasmids was affected by the type of competing plasmids cotransfected in B16-BL6 cells (Fig. 3). Moreover, co-transfection of siRL with pFL-CMV (monitoring plasmid) and pRL-CMV (competing plasmid) significantly rescued FL protein expression compared with the co-transfection of siGFP with pFL-CMV and pRL-CMV. These experimental results suggest for the first time that the translational process is highly likely to be saturated when a large amount of protein is produced. A careful comparison of the results showed that FL expression in the cells

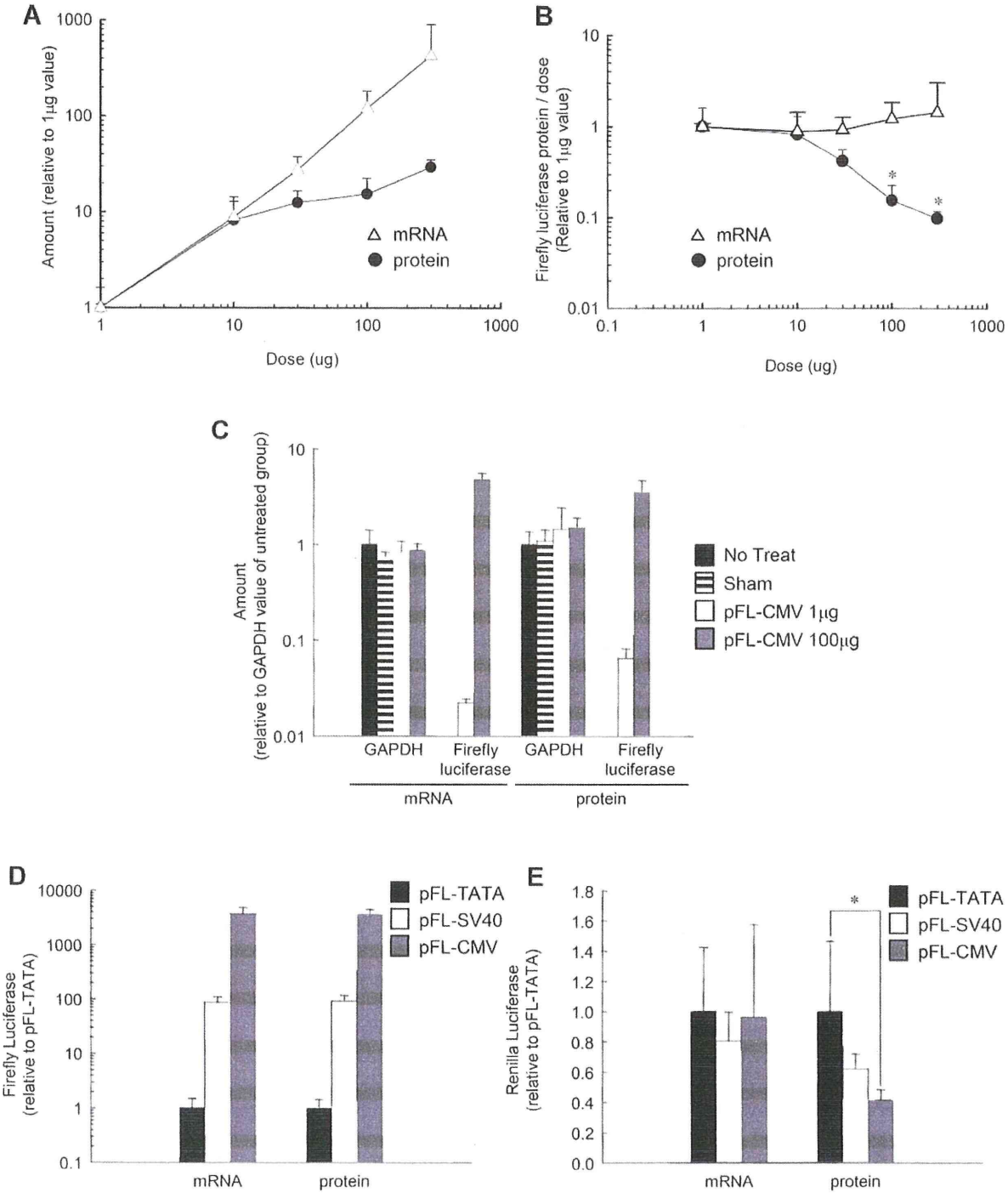

Figure 5. Effect of level of transgene expression from competing plasmid DNA on the expression from monitoring plasmid DNA and endogenous gene in mouse liver. **A**: Mice received a hydrodynamic injection of pFL-CMV at indicated doses. At 6 h after injection, the level of mRNA (open triangle) and protein (closed circle) expression of firefly luciferase were simultaneously measured. The results are expressed as the mean + SD ($n = 4$). **B**: The amount of mRNA or protein expression in (A) was divided by the dose. The results are expressed as the mean + SD of the relative value to that of 1 μg group ($n = 4$). $^*P < 0.05$ versus 1 μg group. **C**: Mice received a hydrodynamic injection of 0 (hatched bar), 1 (open bar), or 100 μg pFL-CMV (gray bar) or were untreated (closed bar). At 6 h after injection, the level of mRNA and protein expression of firefly luciferase and GAPDH were simultaneously measured. The results are expressed as mean ± SD of the relative value to that of GAPDH of the no treatment groups ($n = 4$). **D and E**: Mice received a hydrodynamic injection of 1 μg pRL-CMV and 10 μg pFL-TATA (closed bar), pFL-SV40 (open bar), or pFL-CMV (gray bar). At 6 h after injection, mRNA and protein expression of firefly (C) and renilla (D) luciferase were simultaneously measured. The results are expressed as the mean ± SD ($n = 4$). $^*P < 0.05$.

transfected with pFL-CMV was lower when cells were cotransfected with siRL and pRL-CMV than that with siRL and pRL-TK. As RL amount of the siRL/pFL-CMV/pRL-CMV group was much higher than that of the siRL/pFL-CMV/pRL-TK group, a simple explanation is that siRL-mediated reduction in renilla mRNA was not enough to completely rescue the FL expression. We found a reduced mRNA expression of FL in the pFL-CMV/pRL-CMV group compared to the pFL-CMV/pRL-TK group (Fig. 3B). In addition, siRNA degrades its target mRNA in the cytoplasm so that siRNA does not affect the earlier processes such as transcription. Therefore, the siRL-mediated incomplete rescue of FL protein expression may suggest that not only translation but also the earlier processes such as transcription are also saturated under the experimental conditions used.

The studies using mice led to a slightly different conclusion. Transgene expression was also saturated when a large amount of plasmid DNA was delivered, but the transcription was hardly affected by the dose (Fig. 5A). Therefore, the translational process is likely to be saturated in mouse liver (Fig. 5C and D), which is different from the in vitro results. This apparent discrepancy might be due to the difference in the type of transgene-expressing cells or in the delivery method of plasmid DNA. Further studies are needed to identify factors explaining the discrepancy. The firefly gene sequence in pFL-CMV was not fully codon-optimized for expression in mice and 5% of the codons in the sequence are ones with low frequency (<30%) in mice, so this could be a bottleneck during translation. To our knowledge, no previous study has reported the saturation of transgene expression processes in vivo. Our finding agrees with the results of Carpentier et al. (2007). They found that transcriptional and translational processes are saturated under optimal transfection conditions in which cells were very efficiently transfected with plasmids. In addition, they reported that the translational process is saturated at a dose of plasmid DNA that does not affect the transcriptional process. In the present study, we found that transgene expression process can be saturated when the large amount of plasmid DNA is delivered to mouse liver by hydrodynamic injection. We and others also found a similar phenomenon in lipoplex-mediated and polyplex-mediated transfection of cultured cells, where the mode of gene delivery is different from the hydrodynamic injection (Carpentier et al., 2007). In addition, it has been reported that there is a saturation in secretory pathway after the transfection by adenoviral vectors encoding secretory proteins (Marmorstein et al., 2000). Therefore, we believe that transgene expression could be saturated when cells are transfected using gene vectors with strong promoters.

When the transcription of endogenous genes is inhibited by adenovirus vectors because of the sharing of transcription factors, the expression of endogenous genes was inhibited at the mRNA level, and cells were damaged (Lin et al., 2007). As we observed saturation in the translational process, but not in the transcriptional process, this "promoter squelching" will not be the case. Regarding toxicity, we did not observe any B16-BL6 cell death at 24 h after transfection. As an earlier study by Lin et.al reported that cellular toxicity by promoter squelching was observed at 48 and 72 h after transfection but not at 24 h after transfection, any toxicity in B16-BL6 cells might be observed at later time points. At least 6 h after the hydrodynamic delivery of plasmid DNA, no changes in the mRNA and protein amount of model endogenous gene, GAPDH, was observed. In addition, no damage was observed in the liver of mice at 6 h after hydrodynamic injection. In the case of hydrodynamic gene transfer, peak time of the transgene expression is usually about 6–24 h and transgene expression level declines after the peak time. Therefore, transgene expression after hydrodynamic gene delivery is considered to be not long enough to affect endogenous gene expression.

In conclusion, we demonstrated that the transgene expression process can be saturated both in cultured cells and in mouse liver and that translation is a major process that can be saturated in transgene expression. Therefore, such an approach that can potentiate the gene expression processes of cells such as transcription and translation would be desirable to achieve higher gene expression if the delivery efficiency is high enough to saturate gene expression machinery.

This work was supported in part by Grants-in-Aid for Scientific Research from the Ministry of Education, Science, Sports, and Culture of Japan, by grants from the Ministry of Health, Labour, and Welfare of Japan, and by a grant from the Program for Promotion of Fundamental Studies in Health Sciences of the National Institute of Biomedical Innovation (NIBIO).

References

Carpentier E, Paris S, Kamen AA, Durocher Y. 2007. Limiting factors governing protein expression following polyethylenimine-mediated gene transfer in HEK293-EBNA1cells. J Biotechnol 128(2):268–280.

Cohen RN, van der Aa MAEM, Macaraeg N, Lee AP, Szoka FC Jr. 2009. Quantification of plasmid DNA copies in the nucleus after lipoplex and polyplex transfection. J Controlled Release 135(2):166–174.

Dean DA. 1997. Import of plasmid DNA into the nucleus is sequence specific. Exp Cell Res 230(2):293–302.

Dean DA, Dean BS, Muller S, Smith LC. 1999. Sequence requirements for plasmid nuclear import. Exp Cell Res 253(2):713–722.

Herweijer H, Wolff JA. 2007. Gene therapy progress and prospects: Hydrodynamic gene delivery. Gene Therapy 14(2):99–107.

Kobayashi N, Nishikawa M, Hirata K, Takakura Y. 2004. Hydrodynamics-based procedure involves transient hyperpermeability in the hepatic cellular membrane: Implication of a nonspecific process in efficient intracellular gene delivery. J Gene Med 6(5):584–592.

Kobayashi N, Nishikawa M, Takakura Y. 2005. The hydrodynamics-based procedure for controlling the pharmacokinetics of gene medicines at whole body, organ and cellular levels. Adv Drug Delivery Rev 57(5): 713–731.

Lewis DL, Wolff JA. 2007. Systemic siRNA delivery via hydrodynamic intravascular injection. Adv Drug Delivery Rev 59(2–3):115–123.

Lin H, McGrath J, Wang P, Lee T. 2007. Cellular toxicity induced by SRF-mediated transcriptional squelching. Toxicol Sci 96(1):83–91.

Liu F, Song YK, Liu D. 1999. Hydrodynamics-based transfection in animals by systemic administration of plasmid DNA. Gene Therapy 6(7):1258–1266.

Marmorstein AD, Csaky KG, Baffi J, Lam L, Rahaal F, Rodriguez-Boulan E. 2000. Saturation of, and competition for entry into, the apical secretory pathway. Proc Natl Acad Sci USA 97(7):3248–3253.

Miller AM, Dean DA. 2008. Cell-specific nuclear import of plasmid DNA in smooth muscle requires tissue-specific transcription factors and DNA sequences. Gene Therapy 15(15):1107–1115.

Nomura T, Yasuda K, Yamada T, Okamoto S, Mahato RI, Watanabe Y, Takakura Y, Hashida M. 1999. Gene expression and antitumor effects following direct interferon (IFN)-γ gene transfer with naked plasmid DNA and DC-chol liposome complexes in mice. Gene Therapy 6(1): 121–129.

Poste G, Doll J, Hart IR, Fidler IJ. 1980. In vitro selection of murine B16 melanoma variants with enhanced tissue-invasive properties. Cancer Res 40(5):1636–1644.

Tachibana R, Harashima H, Ide N, Ukitsu S, Ohta Y, Suzuki N, Kikuchi H, Shinohara Y, Kiwada H. 2002. Quantitative analysis of correlation between number of nuclear plasmids and gene expression activity after transfection with cationic liposomes. Pharm Res 19(4):377–381.

Takahashi Y, Nishikawa M, Kobayashi N, Takakura Y. 2005. Gene silencing in primary and metastatic tumors by small interfering RNA delivery in mice: Quantitative analysis using melanoma cells expressing firefly and sea pansy luciferases. J Controlled Release 105(3):332–343.

JVI
Journals.ASM.org

Establishment of a Novel Permissive Cell Line for the Propagation of Hepatitis C Virus by Expression of MicroRNA miR122

Hiroto Kambara,[a] Takasuke Fukuhara,[a] Mai Shiokawa,[a] Chikako Ono,[a] Yuri Ohara,[a] Wataru Kamitani,[b] and Yoshiharu Matsuura[a]
Department of Molecular Virology[a] and Global COE Program,[b] Research Institute for Microbial Diseases, Osaka University, Osaka, Japan

The robust cell culture systems for hepatitis C virus (HCV) are limited to those using cell culture-adapted clones (HCV in cell culture [HCVcc]) and cells derived from the human hepatoma cell line Huh7. However, accumulating data suggest that host factors, including innate immunity and gene polymorphisms, contribute to the variation in host response to HCV infection. Therefore, the existing *in vitro* systems for HCV propagation are not sufficient to elucidate the life cycle of HCV. A liver-specific microRNA, miR122, has been shown to participate in the efficient replication of HCV. In this study, we examined the possibility of establishing a new permissive cell line for HCV propagation by the expression of miR122. A high level of miR122 was expressed by a lentiviral vector placed into human liver cell lines at a level comparable to the endogenous level in Huh7 cells. Among the cell lines that we examined, Hep3B cells stably expressing miR122 (Hep3B/miR122) exhibited a significant enhancement of HCVcc propagation. Surprisingly, the levels of production of infectious particles in Hep3B/miR122 cells upon infection with HCVcc were comparable to those in Huh7 cells. Furthermore, a line of "cured" cells, established by elimination of HCV RNA from the Hep3B/miR122 replicon cells, exhibited an enhanced expression of miR122 and a continuous increase of infectious titers of HCVcc in every passage. The establishment of the new permissive cell line for HCVcc will have significant implications not only for basic HCV research but also for the development of new therapeutics.

Hepatitis C virus (HCV) infects over 170 million people worldwide and frequently leads to persistent infection, which in turn can lead to chronic hepatitis, cirrhosis, and hepatocellular carcinoma (34). HCV belongs to the *Flaviviridae* family and has a single-stranded positive RNA genome of approximately 9.6 kb. The genome of HCV is translated into a single polyprotein at the endoplasmic reticulum (ER) membrane and is then cleaved by host- and virus-encoded proteases, resulting in 10 structural and nonstructural proteins (41, 44). Due to the lack of a small-animal model and an efficient cell culture system, efforts to understand the HCV life cycle as well as development of anti-HCV drugs have been hampered (42). In a major breakthrough, HCV replicon cells, in which HCV RNA autonomously replicates, were established by Lohmann et al. (37). Afterwards, the infectious HCV in cell culture (HCVcc), based on the genotype 2a JFH1 strain in combination with the human hepatocellular carcinoma cell line Huh7, was developed (36, 64, 70). On the basis of the results obtained with these *in vitro* systems, the life cycle of HCV was clarified, and substantial progress has been made in screening host factors involved in HCV propagation as well as anti-HCV drug candidates (20, 51). Among them, a liver-specific microRNA (miRNA), miR122, has been shown to be one of the most important host factors for HCV replication.

miRNAs are small noncoding RNAs that consist of 20 to 25 nucleotides and modulate gene expression in plants and animals (3, 26). Most miRNAs negatively regulate translation through interaction with the 3′ untranslated region (UTR) of mRNA in a sequence-specific manner. Some of them have been shown to play important roles in the viral life cycle (56). Interestingly, miR122 has been shown to bind to HCV 5′ UTRs and to enhance translation and replication of HCV RNA (23, 28, 29, 38, 52). In addition, enhancement of HCVcc propagation through the direct interaction of miR122 with HCV 5′ UTR has been demonstrated (27). Recently, intravenous administration of the locked nucleic acid (LNA) complementary to miR122 was shown to suppress the propagation of HCV in chimpanzees chronically infected with HCV, suggesting that miR122 is a promising therapeutic target for chronic hepatitis C (31).

It has been shown that HCV exploits various host factors to form a replication complex for efficient replication (43). *In vitro* propagation of HCV is limited to Huh7 cells and their derivatives, and thus, it is important to confirm the data obtained in Huh7 cells by using other human liver cell lines, because the patterns of gene expression vary among cell lines. Although establishment of an HCV replicon system based on liver cell lines has been reported (11, 66), robust propagation of HCVcc in well-characterized human liver cell lines other than Huh7 cells has not succeeded yet. The gene expression profile of mice xenotransplanted with human hepatocytes from different donors inoculated with a single source of HCV revealed that host factors contributed to the variation in host response to HCV infection, including the activation of innate antiviral signaling pathways (65). Furthermore, gene polymorphism in interleukin 28B (IL-28B) was shown to be associated with natural clearance (62) and response to combination therapy with interferon (IFN) and ribavirin (19, 58, 59). Therefore, the solely available *in vitro* propagation system for HCVcc, employing Huh7-derived cells, is not sufficient. The establishment of alternative HCV strains and permissive cell lines is needed to elucidate molecular mechanisms of propagation and pathogenesis of HCV in more detail.

Although there have been several attempts to generate chime-

Received 18 September 2011 Accepted 11 November 2011
Published ahead of print 23 November 2011
Address correspondence to Yoshiharu Matsuura, matsuura@biken.osaka-u.ac.jp.
H. Kambara and T. Fukuhara contributed equally to this article.

doi:10.1128/JVI.06242-11

ric HCVs based on the JFH1 strain (21) and an infectious clone of genotype 1a, H77S, that produces fewer infectious particles than the genotype 2a JFH1 strain (68), propagation of HCV was still limited to Huh7 cells. Exogenous expression of miR122 has been shown to support HCV RNA replication in a human embryonic kidney epithelial cell line and mouse embryonic fibroblasts (7, 35), and we therefore thought that the possibility of complete propagation of HCVcc in various human liver cell lines by the expression of miR122 needed to be examined. Among the cell lines that we examined, Hep3B cells, which were established from human liver tumor biopsy samples in 1976 (1) and have been well characterized as model liver cells in various fields of research (47, 55, 63, 67), were shown to support the efficient propagation of HCVcc comparable to that in Huh7 cells by the expression of miR122. Establishment of novel cell culture systems through the exogenous expression of miR122 provides a clue to understanding the precise roles of miR122 in the life cycle of HCV.

MATERIALS AND METHODS

Plasmids. The cDNA clones of wild-type miR122 (WT-miR122), single mutant miR122 (sMT-miR122), double mutant miR122 (dMT-miR122), *Aequorea coerulescens* green fluorescent protein (AcGFP), and claudin-1 (CLDN) were inserted between the XhoI and XbaI sites of a lentiviral vector, pCSII-EF-RfA, which was kindly provided by M. Hijikata, and the resulting plasmids were designated pCSII-EF-WT-miR122, pCSII-EF-sMT-miR122, pCSII-EF-dMT-miR122, pCSII-EF-AcGFP, and pCSII-EF-Claudin1, respectively. pHH-JFH1 was kindly provided by T. Wakita (39). pHH-JFH1-E2p7NS2mt contains three adaptive mutations in pHH-JFH1 (53). pFGR-JFH1 and pSGR-JFH1 encoded a full-length and a subgenomic cDNA of the JFH1 strain, respectively. The complementary sequence of miR122 was inserted into the PmeI site of the pmirGLO vector (Promega, Madison, WI), and the resulting plasmid was designated pmirGLO-miR122comp. pIFNβ-Luc and pISRE-Luc carrying a firefly luciferase gene under the control of the beta IFN (IFN-β) and interferon-sensitive response element (ISRE) promoters, respectively, were kindly provided by T. Kawai and S. Akira. The internal control plasmid encoding a *Renilla* luciferase (pRL-TK) was purchased from Promega. The plasmids used in this study were confirmed by sequencing with an ABI Prism 3130 genetic analyzer (Applied Biosystems, Tokyo, Japan).

Cells. All cell lines were cultured at 37°C under the condition of a humidified atmosphere and 5% CO_2. The human embryonic kidney 293T cell line and hepatocellular carcinoma cell lines Huh7, Huh6/CLDN, HepG2/CD81, Hep3B, and PKC/PRL/5 were maintained in Dulbecco's modified Eagle's medium (DMEM; Sigma, St. Louis, MO) supplemented with 100 U/ml penicillin, 100 μg/ml streptomycin, and 10% fetal calf serum (FCS). HepG2/CD81 cells were generated as described previously (60). Huh6 cells were transduced with a lentiviral vector expressing claudin-1, and the resulting cells were designated Huh6/CLDN. The Huh7-derived cell line Huh7.5.1 was kindly provided by F. Chisari and was maintained in DMEM containing nonessential amino acids (NEAA), 100 U/ml penicillin, 100 μg/ml streptomycin, and 10% FCS. Hep3B replicon cells harboring the subgenomic HCV RNA were maintained in DMEM containing 10% FCS, NEAA, and 400 μg/ml G418 (Nakalai Tesque, Kyoto, Japan).

Viruses. pHH-JFH1-E2p7NS2mt was transfected into Huh7.5.1 cells, and the culture supernatants were collected after serial passages. The infectivity of HCVcc was determined by focus-forming assay and expressed in focus-forming units (FFU) (64). The lentiviral vectors and ViraPower lentiviral packaging mix (Invitrogen, San Diego, CA) were cotransfected into 293T cells, and the supernatants were recovered at 48 h posttransfection. The culture supernatants were centrifuged at 1,000 $\times$ *g* for 5 min and cleared through a 0.45-μm-pore-size filter. The lentivirus titer was determined by a Lenti-X quantitative reverse transcription (qRT)-PCR titration kit (Clontech, Mountain View, CA). The vesicular stomatitis virus (VSV) variant NCP12.1, derived from the Indiana strain, was kindly provided by M. Whitt. Pseudotype VSVs bearing the HCV E1 and E2 glycoproteins (HCVpv) and VSV G protein (VSVpv) were prepared as described previously (60). The infectivity of the pseudotype viruses was assessed by the expression of luciferase, determined by a Bright-Glo luciferase assay system (Promega) following a protocol provided by the manufacturer and expressed in relative light units (RLU).

Reagents and antibodies. Cyclosporine (CsA) and human recombinant IFN-α2 were purchased from Sigma and R&D Systems (Minneapolis, MN), respectively. BODIPY 558/568 lipid probe was purchased from Invitrogen. Poly(I·C) was purchased from InvivoGen (San Diego, CA). LNAs complementary to miR122 (LNA-miR122; 5′-CcAttGTcaCaCtCC-3′) and its negative control (LNA-Cont; 5′-CcAttCTgaCcCtAC-3′) (LNA in capital letters, DNA in lowercase letters; sulfur atoms in oligonucleotide phosphorothioates are substituted for nonbridging oxygen atoms; capital C indicates LNA methylcytosine) (14) were purchased from Gene Design (Osaka, Japan). miScript miRNA mimics hsa-miR122 and its negative control were purchased from Qiagen (Valencia, CA). Mouse monoclonal antibodies to HCV NS5A and β-actin were purchased from Austral Biologicals (San Ramon, CA) and Sigma, respectively. Mouse anti-apolipoprotein E (anti-ApoE), rabbit anti-diacylglycerol acyltransferase 1 (DGAT1), rabbit anti-signal transducer and activators of transcription 2 (anti-STAT2), and rabbit anti-IFN regulatory factor 3 (anti-IRF3) antibodies were purchased from Santa Cruz (Santa Cruz, CA). Rabbit anti-HCV core protein was prepared as described previously (45). Phycoerythrin (PE)-conjugated anti-human CD81 (anti-hCD81) and anti-mouse IgG antibodies were purchased from BD Biosciences (Franklin Lakes, NJ). Mouse anti-double-stranded RNA (anti-dsRNA) IgG2a (J1 and K2) antibodies were from Biocenter Ltd. (Szirak, Hungary). Alexa Fluor 488 (AF488)-conjugated anti-mouse and -rabbit IgG and AF594-conjugated anti-rabbit IgG antibodies were from Invitrogen.

Quantitative RT-PCR. For quantitation of HCV RNA, total RNA was prepared from cells by using an RNeasy minikit (Qiagen). The synthesis of a first-stranded cDNA and quantitative RT-PCR were performed using TaqMan EZ RT-PCR core reagents and an ABI Prism 7000 system (Applied Biosystems) according to the manufacturer's protocol. For quantitation of miRNA, total RNA was prepared from cells by using an miRNeasy minikit (Qiagen), and miR122 was estimated by using miR122-specific RT primers and amplified using specific primers provided in the TaqMan MicroRNA assays (Applied Biosystems) according to the manufacturer's protocol. U6 small nuclear RNA (snRNA) was used as an internal control. Fluorescent signals were analyzed by an ABI Prism 7000 system (Applied Biosystems).

Transfection and immunoblotting. Cells were transfected with the plasmids by using *Trans* IT LT-1 (Mirus, Madison, WI) or Lipofectamine 2000 (Invitrogen) according to the manufacturers' protocols. Cells were lysed on ice in Triton lysis buffer (20 mM Tris-HCl [pH 7.4], 135 mM NaCl, 1% Triton X-100, 10% glycerol) supplemented with a protease inhibitor mix (Nacalai Tesque). The samples were boiled in loading buffer and subjected to 5 to 20% gradient sodium dodecyl sulfate-polyacrylamide gel electrophoresis (SDS-PAGE). The proteins were transferred to polyvinylidene difluoride membranes (Millipore, Bedford, MA) and reacted with primary antibody and then secondary horseradish peroxidase-conjugated antibody. The immunocomplexes were visualized with Super Signal West Femto substrate (Pierce, Rockford, IL) and detected by using an LAS-3000 image analyzer (Fujifilm, Tokyo, Japan).

Indirect immunofluorescence assay. Cells cultured on glass slides were fixed with 4% paraformaldehyde in phosphate-buffered saline (PBS) at room temperature for 30 min. After washing three times with PBS, the cells were permeabilized for 20 min at room temperature with PBS containing 0.25% saponin and blocked with phosphate buffer containing 2% bovine serum albumin (BSA) for 1 h at room temperature. The cells were incubated with blocking buffer containing mouse anti-dsRNA, rabbit anti-NS5A, rabbit anti-core, rabbit anti-IRF3, or rabbit anti-STAT2 at room temperature for 1 h, washed three times with PBS, and incubated

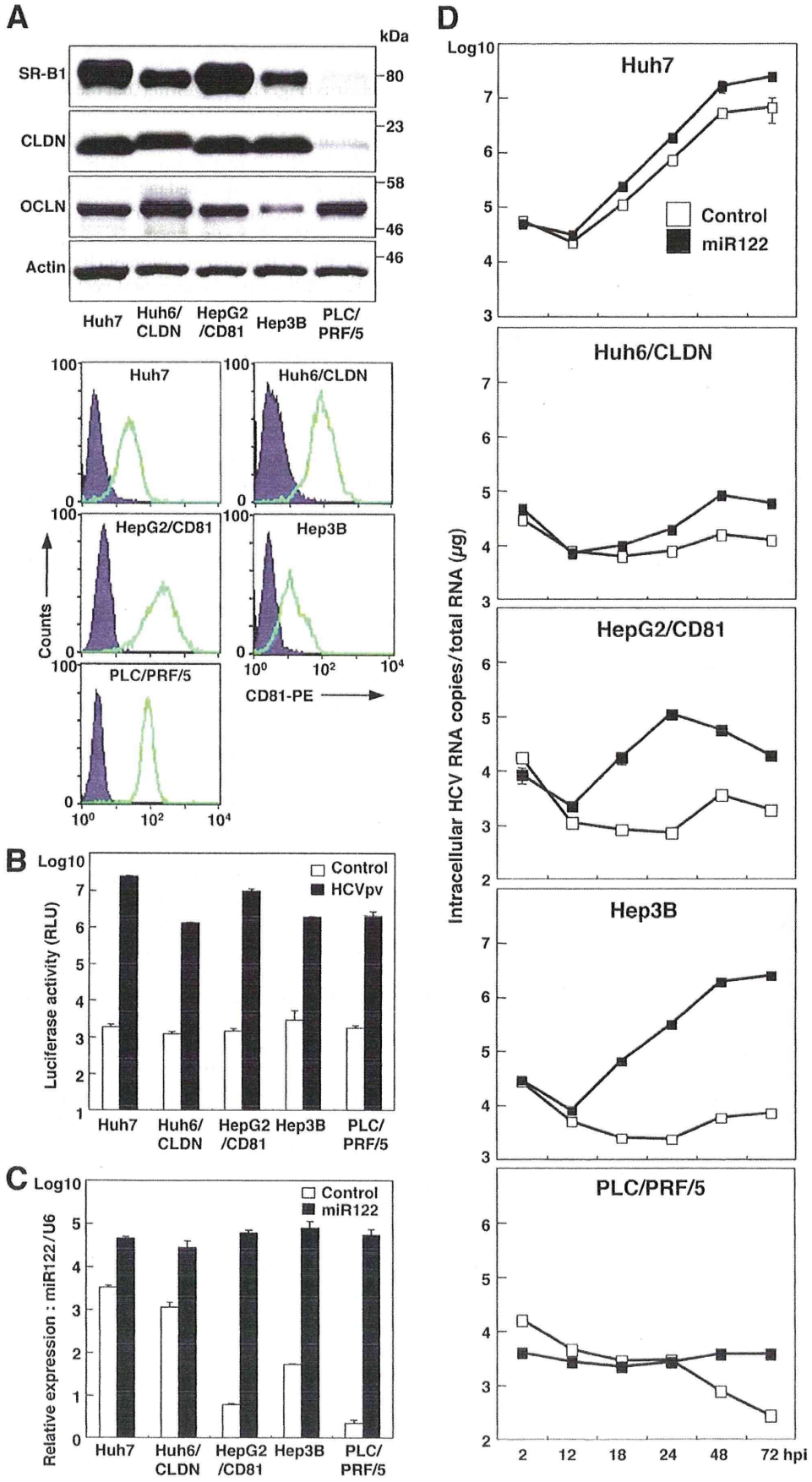

with blocking buffer containing appropriate AF488-conjugated and AF594-conjugated secondary antibodies at room temperature for 1 h. Finally, the cells were washed three times with PBS and observed with a FluoView FV1000 laser scanning confocal microscope (Olympus, Tokyo, Japan).

Flow cytometry. Cultured cells were detached with 0.25% trypsin-EDTA and incubated with PE-conjugated anti-hCD81 antibody or anti-mouse IgG antibody for 1 h at 4°C. After being washed twice with PBS containing 1% BSA, the cells were analyzed by a BD FACSCalibur flow cytometry system (BD Biosciences).

***In vitro* transcription, RNA transfection, and colony formation.** The plasmids pSGR-JFH1 and pFGR-JFH1 were linearized with XbaI and treated with mung bean exonuclease. The linearized DNA was transcribed *in vitro* by using a MEGAscript T7 kit (Applied Biosystems) according to the manufacturer's protocol. The *in vitro*-transcribed RNA (10 μg) was electroporated into Hep3B cells at 10^6 cells/0.4 ml under conditions of 270 V and 960 μF using a Gene Pulser apparatus (Bio-Rad, Hercules, CA) and plated on DMEM containing 10% FCS and NEAA. The medium was replaced with fresh DMEM containing 10% FCS, NEAA, and 400 μg/ml G418 at 24 h posttransfection. The remaining colonies were fixed with 4% paraformaldehyde and stained with crystal violet at 1 month postelectroporation.

Luciferase assay. Cells were seeded onto 24-well plates at a concentration of 5×10^4 cells/well and transfected with 250 ng of each of the plasmids. At 24 h posttransfection, cells were stimulated with the appropriate ligands for 24 h and then lysed in 100 μl of passive lysis buffer (Promega). Luciferase activity was measured in 20-μl aliquots of the cell lysates using a dual-luciferase reporter assay system (Promega). Firefly luciferase activity was standardized with that of *Renilla* luciferase cotransfected with the internal control plasmid pRL-TK and was expressed as RLU.

RESULTS

Expression of miR122 facilitates replication of HCVcc in various liver cell lines. The robust *in vitro* cell culture systems for HCV use the HCV genotype 2a isolate JFH1 and Huh7-derived cell lines (64). To expand the host range of HCVcc to gain more insight into the host-virus interaction, we examined the effect of expression of miR122, a liver-specific microRNA that was shown to be crucial for the efficient replication of HCV (27–29, 38, 52), in several well-characterized liver cell lines: Huh6, HepG2, Hep3B, and PLC/PRF/5. Although hCD81, SR-B1, claudin-1 (CLDN), and occludin (OCLN) are known to be crucial for entry of HCVcc (15, 48, 49, 54), the Huh6 and HepG2 cell lines express little or no CLDN and hCD81 (10, 22), respectively. Therefore, CLDN and hCD81 were exogenously expressed in the cell lines, and the resulting lines were designated Huh6/CLDN and HepG2/CD81, respectively. Expression of the receptor molecules in the cell lines was confirmed by immunoblot and fluorescence-activated cell sorter (FACS) analyses (Fig. 1A). To further examine the susceptibility to HCV infection, pseudotyped VSV bearing the HCV envelope protein, HCVpv, was inoculated into these cell lines. Significant expression of luciferase was observed in these cell lines upon infection with HCVpv but not upon infection with the control virus (Fig. 1B), suggesting that the liver cell lines express functional receptors required for entry of HCV. To determine the effect of miR122 on the replication of HCVcc, we next assessed the level of miR122 in the liver cell lines by qRT-PCR. Although miR122 is highly expressed in the liver (13), the expression level of miR122 varied among the liver cell lines (Fig. 1C, white bars). To examine the effect of the exogenous expression of miR122 in the liver cell lines on the replication of HCVcc, miR122 was expressed in the cell lines by the lentiviral vector. The expression level of miR122 in the liver cell lines, including Huh7 cells, was shown to be upregulated to a significantly greater extent than that in Huh7 cells alone (Fig. 1C, black bars). To examine the effect of miR122 on the replication of HCV, HCVcc was inoculated into the cell lines (Fig. 1D). Although Huh7 cells exhibited an efficient HCV replication, a slight enhancement of the replication was observed by the expression of miR122. No HCV replication was observed in PLC/PRF/5 cells irrespective of miR122 expression. Hep3B and HepG2/CD81 cells exhibited a significant enhancement of HCV replication by the expression of miR122, in contrast to a slight increase in Huh6/CLDN cells. Notably, HCV RNA levels were drastically increased by more than 300-fold at 72 h postinfection in Hep3B cells by the expression of miR122, suggesting that Hep3B is the most suitable cell line for investigating the biological significance of miR122 on the propagation of HCV and for establishing a permissive cell line for HCVcc. Therefore, we used Hep3B cells overexpressing miR122 (Hep3B/miR122 cells) for further experiments.

Expression of biologically active miR122 facilitates replication of HCVcc in Hep3B cells. To confirm the activity of endogenously and exogenously expressed miR122 to suppress the translation in cells, a pmirGLO vector carrying the complementary sequence of miR122 under the luciferase gene was transfected into Huh7 cells, Hep3B cells expressing AcGFP (Hep3B/Cont), and Hep3B/miR122 cells. Suppression of luciferase expression was observed in Huh7 and Hep3B/miR122 cells but not in Hep3B/Cont cells (Fig. 2A), suggesting that miR122 exogenously expressed in Hep3B cells is as biologically active as that endogenously expressed in Huh7 cells. To determine the effect of miR122 on the propagation of HCVcc, Hep3B cells were infected with the lentiviral vector expressing miR122 and then inoculated with HCVcc. The levels of HCV RNA in Hep3B cells upon infection with HCVcc were increased in proportion to the amount of lentiviral vector (Fig. 2B). Recently, an inhibitor for miR122, SPC3649, which is an LNA in which 2′ oxygen and 4′ carbon are connected via methylene units, has been shown to possess potent anti-HCV activity in chimpanzees chronically infected with HCV (31). We next examined the effect of LNA on the replication of HCVcc in Huh7 and Hep3B/miR122 cells. HCV RNA replication in Huh7 and Hep3B/miR122 cells was significantly and dose-dependently decreased by treatment with LNA-miR122 but not treatment with LNA-Cont (Fig. 2C). We further investigated the effect of the

FIG 1 Expression of miR122 facilitates replication of HCVcc in various liver cell lines. (A) Human liver cell lines Huh7, Huh6/CLDN, HepG2/CD81, Hep3B, and PLC/PRF/5 were lysed and subjected to immunoblotting using appropriate antibodies. The expression levels of hCD81 in the liver cell lines were determined by flow cytometry. (B) The human liver cell lines were inoculated with HCVpv or control virus and washed three times after 2 h of incubation. Luciferase activities were determined at 24 h postinfection. (C) The cell lines were transduced with lentiviral vectors expressing miR122 or AcGFP as a control. After serial passages, total RNA was extracted from the cells and relative expression of miR122 was determined by qRT-PCR by using U6 snRNA as an internal control. (D) The cells expressing miR122 or control were infected with HCVcc at an MOI of 1. Total RNA was extracted from the cells at the indicated time and subjected to qRT-PCR analysis. The data are representative of three independent experiments. Error bars indicate the standard deviation of the mean.

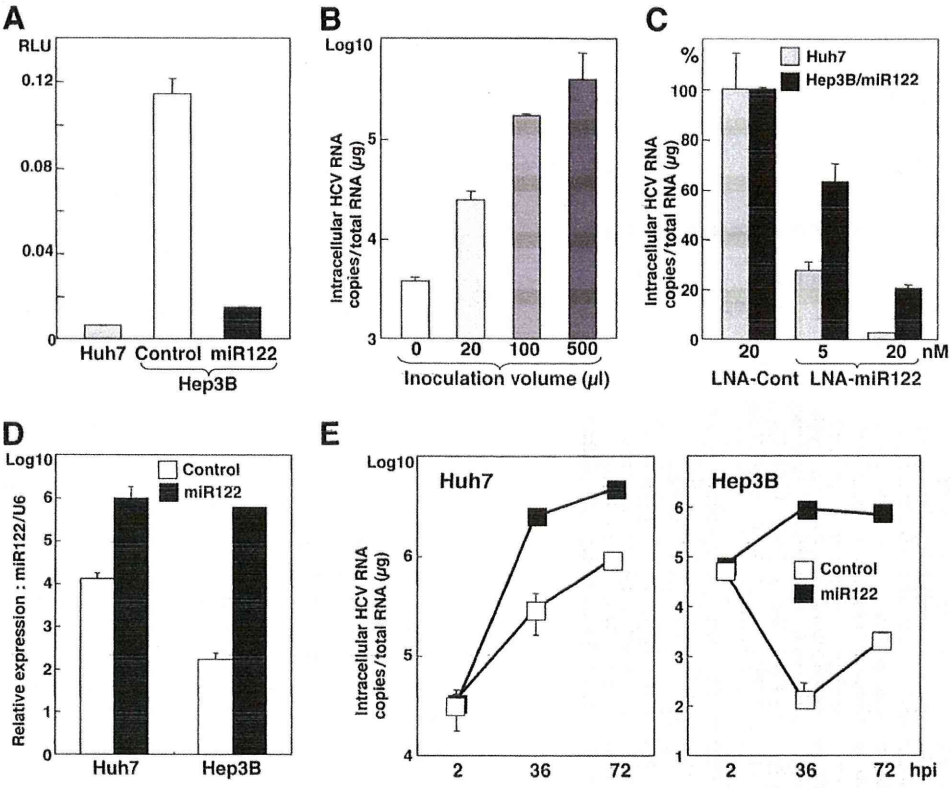

FIG 2 Expression of biologically active miR122 facilitates replication of HCVcc in Hep3B cells. (A) Huh7, Hep3B/Cont, and Hep3B/miR122 cells were transfected with pmirGLO-miR122comp, and luciferase activity was determined at 24 h posttransfection. (B) Hep3B cells were transduced with the lentiviral vector expressing miR122 in a dose-dependent manner and then infected with HCVcc at an MOI of 1 at 48 h postransduction. Total RNA was extracted from the cells at 72 h postinfection and subjected to qRT-PCR. (C) LNA-Cont (20 nM) or LNA-miR122 (5 nM or 20 nM) was introduced into Hep3B/miR122 cells and infected with HCVcc at an MOI of 1 at 12 h posttransfection. Total RNA was extracted from the cells at 24 h postinfection and subjected to qRT-PCR. (D) Huh7 and Hep3B cells were transfected with mimic miR122 (20 nM) or a negative control (20 nM), and total miRNA was determined by qRT-PCR at 24 h posttransfection. (E) Huh7 and Hep3B cells were transfected with mimic miR122 (20 nM) or a negative control (20 nM) and infected with HCVcc at an MOI of 1 at 12 h posttransfection. Total RNA was extracted from the cells at the indicated time (hpi, hours postinfection) and subjected to qRT-PCR.

mimic miR122, the synthetic double-stranded RNA oligonucleotides that mimic endogenous miRNA function, on the propagation of HCV. Huh7 and Hep3B cells transfected with mimic miR122 but not those transfected with the negative control exhibited a high level of expression of miR122 (Fig. 2D) and enhanced RNA replication upon infection with HCVcc (Fig. 2E). Collectively, these results clearly indicate that expression of biologically active miR122 plays a crucial role in the replication of HCV in Hep3B cells.

Establishment of a novel permissive cell line for robust propagation of HCVcc by expression of miR122 in Hep3B cells. We next examined the possibility of establishing a permissive cell line for the robust propagation of HCVcc by the expression of miR122 in Hep3B cells. Huh7, Hep3B/miR122, and Hep3B/Cont cells were infected with HCVcc, and the levels of expression of HCV NS5A and core proteins were assessed by immunoblotting at 72 h postinfection. Expression of the viral proteins in Hep3B/miR122 cells was almost comparable to that in Huh7 cells, in contrast to no expression in Hep3B/Cont cells (Fig. 3A). Small foci stained by immunofluorescence assay appeared at 24 h postinfection in Hep3B/miR122 and Huh7 cells but not in Hep3B/Cont cells and grew into large foci at 72 h postinfection, indicating that infectious particles are generated in Hep3B/miR122 cells and the progeny particles expand infection to the neighboring cells (Fig. 3B). The morphology of Hep3B cells is completely different from that of Huh7 cells, and thus, these results are not due to contamination of Huh7 cells. DGAT1 and ApoE have been shown to play crucial roles in the recruitment of core protein to the lipid droplets and viral infectivity, respectively (9, 24). Higher levels of expression of ApoE and DGAT1 were detected in Hep3B cells than in Huh7 cells (Fig. 3C). Furthermore, the concentration of infectious particles recovered in the culture supernatant of Hep3B/miR122 cells infected with HCVcc at a multiplicity of infection (MOI) of 1 at 72 h postinfection was approximately 5×10^4 FFU/ml, which was comparable to that in Huh7 cells, and was in clear contrast to the significantly lower titer in Hep3B/Cont cells (less than 10 FFU/ml). These results clearly indicate that expression of miR122 in Hep3B cells enables the establishment of a novel permissive cell line for the robust propagation of HCVcc.

Establishment of an HCV RNA replicon in Hep3B/miR122 cells. It has been shown that "cured" cells established through the elimination of the HCV genome from replicon cells by treatment with IFN-α exhibited more potent propagation of HCVcc than the original Huh7 cells (4). To establish a cured cell line derived from Hep3B/miR122 cells for further improvement of HCVcc propagation, we first established HCV replicon cells in Hep3B/miR122 cells. *In vitro*-transcribed sub- or full-genomic HCV RNA of the JFH1 strain was electroporated into Hep3B/miR122 and

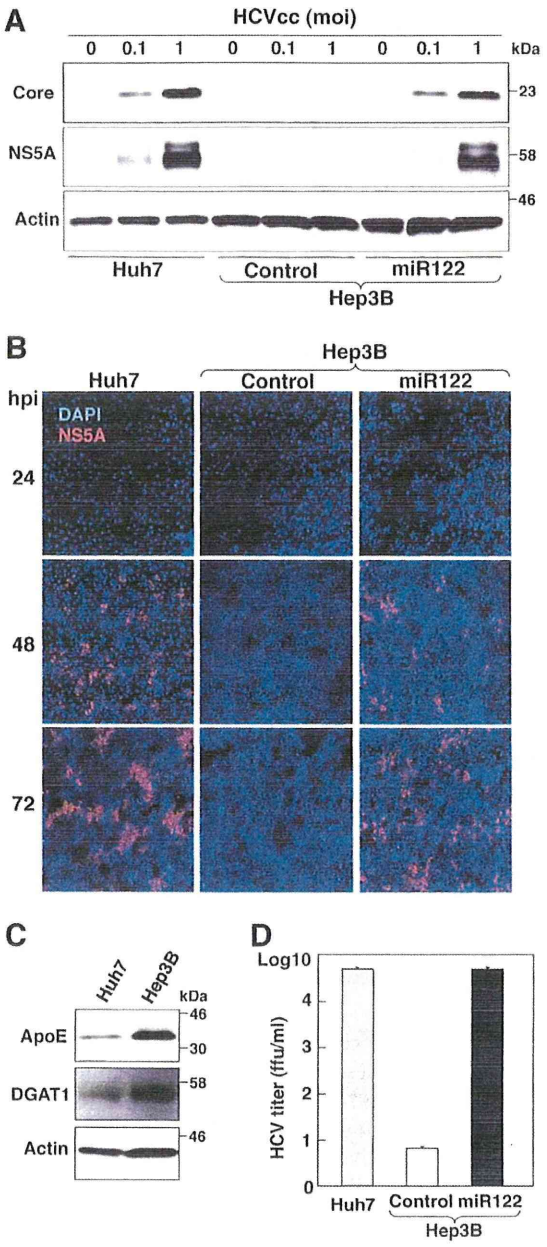

FIG 3 Establishment of a novel permissive cell line for robust propagation of HCVcc by expression of miR122 in Hep3B cells. (A) Huh7, Hep3B/Cont, and Hep3B/miR122 cells were infected with HCVcc at an MOI of 0.1 or 1, and the levels of expression of viral proteins were determined by immunoblotting using appropriate antibodies at 72 h postinfection. (B) Huh7, Hep3B/Cont, and Hep3B/miR122 cells were infected with HCVcc at an MOI of 1 and incubated with 1% methylcellulose in DMEM containing 5% FCS for the indicated time. Cells were fixed with 4% paraformaldehyde and subjected to indirect immunofluorescence assay using anti-NS5A antibody, followed by AF594-conjugated anti-rabbit IgG (red). Cell nuclei were stained with 4′,6-diamidino-2-phenylindole (DAPI; blue). (C) Huh7 and Hep3B cells were lysed and subjected to immunoblotting using appropriate antibodies. (D) Huh7, Hep3B/Cont, and Hep3B/miR122 cells were infected with HCVcc at an MOI of 1, the culture supernatants were collected at 72 h postinfection, and the viral titers of the supernatants were determined by focus-forming assay using Huh7.5.1 cells.

Hep3B/Cont cells, the cells were cultured with 400 μg/ml of G418 for 1 month, and subgenomic replicon (SGR) and full-genomic replicon (FGR) cells were established. Hep3B/miR122 cells electroporated with viral RNA generated a large number of colonies, in contrast to the complete absence of colony formation in Hep3B/Cont cells (Fig. 4A). High levels of HCV RNA comparable to those in the Huh7 cells harboring SGR of the JFH1 strain were detected in Hep3B/miR122 cells harboring either SGR or FGR of the JFH1 strain (Fig. 4B, lower). Expression of NS5A was detected in all of the clones of Hep3B/miR122 cells harboring either SGR or FGR, and that of the core protein was detected in all of the FGR clones (Fig. 4B, upper). HCV core protein and RNA were shown to localize mainly on the lipid droplets and on the cytoplasmic face of ER, respectively (40, 61). Immunofluorescence analyses revealed that dsRNA was colocalized with calnexin, an ER marker, in both SGR and FGR cells and HCV core protein was colocalized with lipid droplets in the FGR cells, as previously described (Fig. 4C). Treatment of Hep3B/miR122 cells harboring an FGR of the JFH1 strain with either CsA or IFN-α decreased the expression of core protein in a dose-dependent manner (Fig. 4D), suggesting that the Hep3B/miR122 replicon cells can be used for screening antiviral compounds for HCV.

Elimination of HCV RNA from HCV replicon RNA from Hep3B/miR122 cells enhances propagation of HCVcc. To establish cured Hep3B/miR122 cells, five clones of the Hep3B/miR122 replicon cells harboring FGR of the JFH1 strain were treated with 100 IU/ml of IFN-α to eliminate viral RNA, and viral RNA was gradually decreased and completely eliminated at 20 days posttreatment (Fig. 5A, left). We then examined the sensitivity of the cured cell clones for propagation of HCVcc. All of the cured cell clones exhibited enhancement of propagation of HCVcc, especially clone 5, which achieved a level of replication of HCVcc more than 6-fold higher than that in the parental Hep3B/miR122 cells (Fig. 5A, right). To examine the effect of serial passage of HCVcc in the cured Hep3B/miR122 cells, HCVcc was inoculated into the cured cells at an MOI of 0.1, and the culture supernatants harvested at 4 days postinfection were reinoculated into the naïve cured cells (Fig. 5B). Infectious titers in the culture supernatants were continuously increased in accord with the number of passages (Fig. 5C). These results indicate that a novel cell line capable of complete propagation of HCVcc was established by the introduction of miR122 and the curing process, as in the case of Huh7 cells by using Hep3B cells.

Cured Hep3B/miR122 cells facilitate efficient propagation of HCVcc through enhanced expression of miR122. It has been reported that one of the reasons for the high susceptibility of the cured cell line Huh7.5 to the propagation of HCVcc is the disruption of the innate immune responses caused by mutation in RIG-I, a key sensor for viral RNA in the cytoplasm (57, 69). To examine the innate immune response in the cured Hep3B/miR122 cells, reporter plasmids encoding the luciferase gene under the control of either the IFN-β (Fig. 6A, left) or ISRE (Fig. 6A, right) promoter were transfected into the cured or parental Hep3B/miR122 cells and stimulated with poly(I·C), VSV, or IFN-α. Activation of these promoters in the cured Hep3B/miR122 cells was not impaired but rather was enhanced upon stimulation with poly(I·C) or VSV compared with that in the parental cells. To further assess the authenticity of viral RNA recognition and ISG induction pathways in the cured Hep3B/miR122 cells, nuclear localization of IRF3 and STAT2 upon stimulation was determined by immuno-

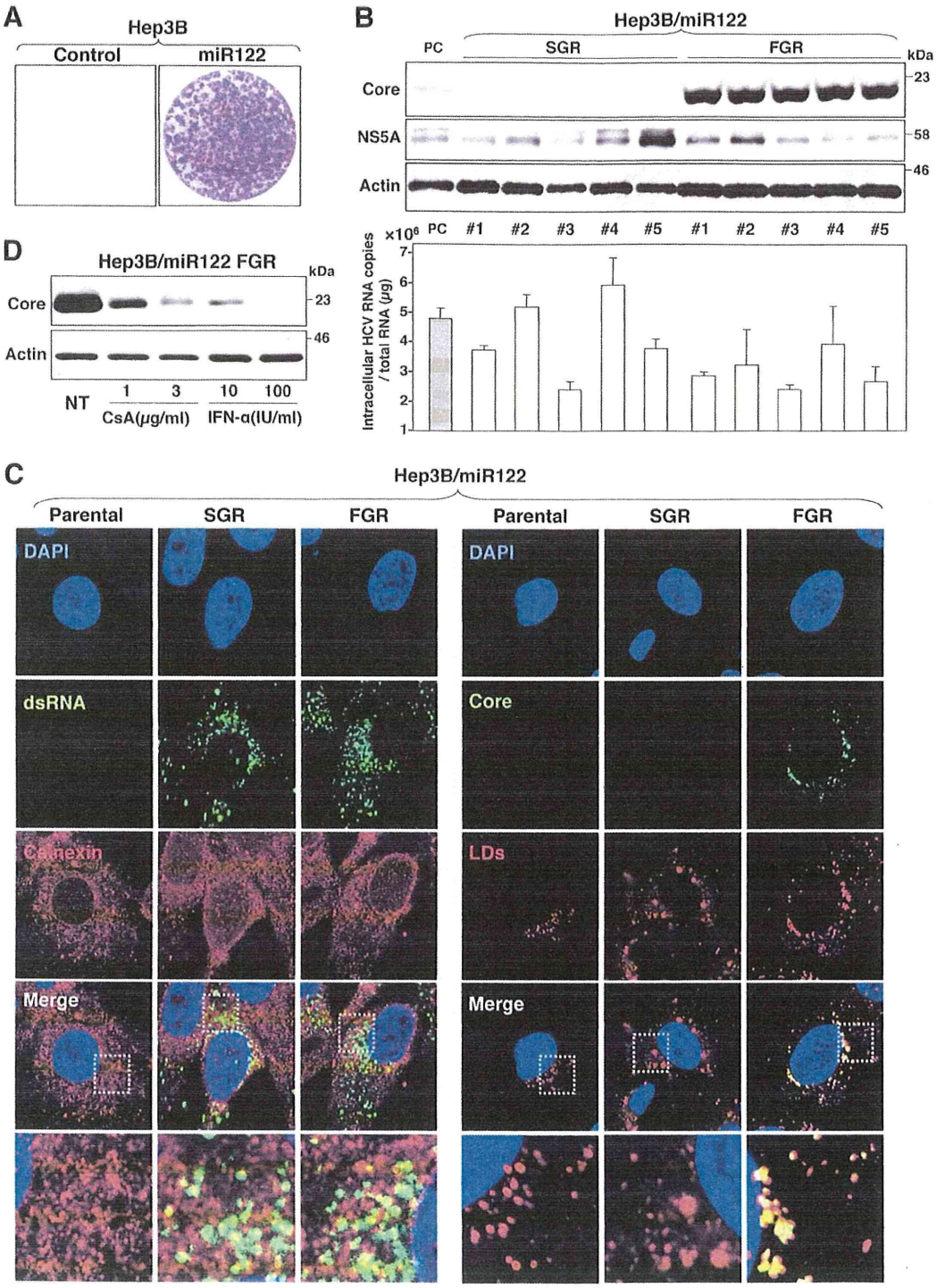

FIG 4 Establishment of an HCV RNA replicon in Hep3B/miR122 cells. (A) Full-genomic replicon RNA of HCV was electroporated into Hep3B/Cont and Hep3B/miR122 cells, and the medium was replaced with DMEM containing 10% FCS and 400 μg/ml G418 at 24 h posttransfection. Colony formation was determined as indicated in Materials and Methods. (B) (Upper) Sub- and full-genomic HCV replicons (SGR and FGR) in Hep3B/miR122 cells were subjected to immunoblotting using the appropriate antibodies. Huh7.5.1 cells infected with HCVcc were used as a positive control (PC). (Lower) Intracellular HCV copy number in replicon clones. SGR in Huh7 cells was used as a positive control. (C) SGR and FGR in Hep3B/miR122 cells were fixed with 4% paraformaldehyde and subjected to indirect immunofluorescence assay using the appropriate antibodies. Lipid droplets (LDs) were stained red with BODIPY. Cell nuclei were stained with 4′,6-diamidino-2-phenylindole (blue). The boxed regions in the merged images are magnified. (D) Hep3B/miR122 FGR cells were treated with DMEM containing 10% FCS and the indicated concentrations of CsA and IFN-α and then subjected to immunoblotting using appropriate antibodies at 48 h posttransfection. NT, no treatment.

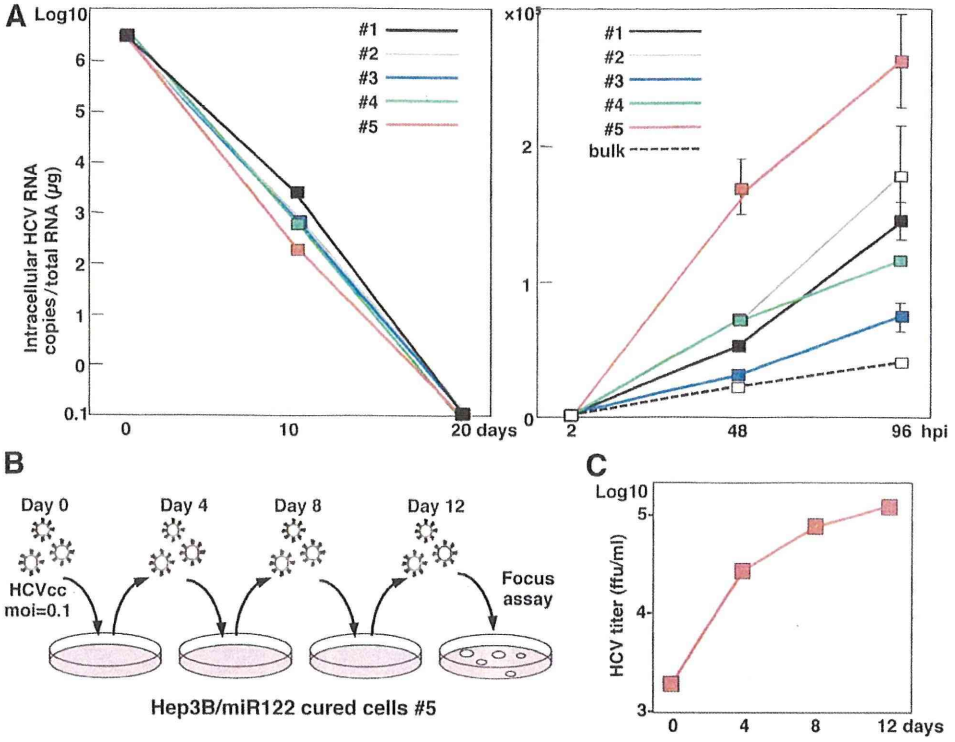

FIG 5 Elimination of HCV RNA from HCV replicon RNA from Hep3B/miR122 cells enhances propagation of HCVcc. (A) (Left) Hep3B/miR122 FGR cell clones were treated with IFN-α (100 IU/ml), and HCV RNA was determined by qRT-PCR at 10 and 20 days posttreatment; (right) Hep3B/miR122 parental cells (bulk) and the cured cells were infected with HCVcc at an MOI of 0.1, and HCV RNA was determined by qRT-PCR at 48 and 96 h postinfection. (B) Schematic diagram of the experimental procedure for serial passage of HCVcc in Hep3B/miR122 cured cells. The cured cells were infected with HCVcc at an MOI of 0.1. (C) The infectious titers in the culture supernatants of the Hep3B/miR122 cured cells were determined at the indicated time points by focus-forming assay using Hep3B/miR122 cells.

fluorescence analysis. IRF3 and STAT2 in both cured and parental Hep3B/miR122 cells were translocated into the nucleus upon stimulation with VSV and IFN-α, respectively (Fig. 6B). These results suggest that the efficient propagation of HCVcc in the cured Hep3B/miR122 cells might be attributable to reasons other than impairment of the innate immune response. Therefore, we hypothesized that the Hep3B/miR122 cells harboring the HCV genome are capable of surviving in the presence of a high concentration of G418 by amplification of the viral genome through enhancement of miR122 expression and that once HCV RNA was eliminated, the cured cells would acquire the ability to propagate HCV due to the high expression of miR122. To test this hypothesis, the levels of miR122 in both Huh7- and Hep3B/miR122-derived cured cells were compared with those in the parental cells. Intriguingly, both cured cell lines exhibited a significant increase of miR122 expression (approximately 2- to 6-fold) in comparison with that in the parental cells (Fig. 6C). These results suggest that the efficient propagation of HCVcc in the cured Hep3B/miR122 cells was partially attributable to an enhanced expression of miR122, rather than an impairment of the signaling pathway of innate immunity.

Specific interaction of miR122 with viral RNA is crucial for efficient propagation of HCVcc. To evaluate the effect of a specific interaction of miR122 with the target sequence in the 5′ UTR of HCV RNA on the enhancement of viral propagation, we generated two mutant pre-miR122s: sMT-miR122 has a substitution of uridine to adenosine, and dMT-miR122 carries an additional complementary substitution of adenosine to uridine to stabilize the expression. These substitutions have been shown to abrogate interaction with the target sequence (27) (Fig. 7A). A high level of expression of dMT-miR122 comparable to that of WT-miR122 was detected in Hep3B cells, in contrast to the low level of expression of sMT-miR122 (Fig. 7B). As described above, the expression level of miR122 in Hep3B cells was significantly lower than that in Huh7 cells (Fig. 1B). Taking advantage of this low level of miR122 expression, WT-miR122 and dMT-miR122 were exogenously expressed in Hep3B cells by the lentiviral vector to assess the importance of the specific interaction of miR122 with viral RNA. Not only intracellular viral RNA levels but also infectious titers in the culture supernatants were enhanced by the expression of WT-miR122, but they were not enhanced by the expression of dMT-miR122 (Fig. 7C and D). These results suggest that specific interaction of miR122 with the 5′ UTR of HCV is crucial for the efficient replication and propagation of HCV.

DISCUSSION

Most miRNAs utilize the normal RNA interfering pathway and repress translation of the target mRNAs (3, 26). For instance, miR122 targets the 3′ UTR of the cytoplasmic polyadenylation element binding protein (CPEB) (5), hemochromatosis (*Hfe*) and hemojuvelin (*Hjv*) (6), a disintegrin and metalloprotease family 10 (ADAM10) (2), and cationic amino transporter 1 (CAT-1) (8) and represses their translation. In contrast, HCV uniquely exploits the liver-specific miR122 to stimulate viral translation (23, 27–29,